# The Arabidopsis Vacuolar Sorting Receptor1 Is Required for Osmotic Stress-Induced Abscisic Acid Biosynthesis[1][OPEN]

**Zhen-Yu Wang, Chris Gehring, Jianhua Zhu, Feng-Min Li, Jian-Kang Zhu, and Liming Xiong***

Biological and Environmental Sciences and Engineering Division, King Abdullah University of Science and Technology, Thuwal 23955–6900, Saudi Arabia (Z.-Y.W., C.G., L.X.); State Key Laboratory of Grassland Agroecosystem, Institute of Arid Agroecology, School of Life Sciences, Lanzhou University, Lanzhou 730000, Gansu Province, China (Z.-Y.W., F.-M.L.); Department of Plant Science and Landscape Architecture, University of Maryland, College Park, Maryland 20742 (J.Z.); Department of Horticulture and Landscape Architecture, Purdue University, West Lafayette, Indiana 47907 (J.-K.Z.); and Shanghai Center for Plant Stress Biology, Shanghai Institutes of Biological Sciences, Chinese Academy of Sciences, Shanghai 200032, China (J.-K.Z.)

Osmotic stress activates the biosynthesis of the phytohormone abscisic acid (ABA) through a pathway that is rate limited by the carotenoid cleavage enzyme 9-cis-epoxycarotenoid dioxygenase (NCED). To understand the signal transduction mechanism underlying the activation of ABA biosynthesis, we performed a forward genetic screen to isolate mutants defective in osmotic stress regulation of the *NCED3* gene. Here, we identified the Arabidopsis (*Arabidopsis thaliana*) Vacuolar Sorting Receptor1 (VSR1) as a unique regulator of ABA biosynthesis. The *vsr1* mutant not only shows increased sensitivity to osmotic stress, but also is defective in the feedback regulation of ABA biosynthesis by ABA. Further analysis revealed that vacuolar trafficking mediated by VSR1 is required for osmotic stress-responsive ABA biosynthesis and osmotic stress tolerance. Moreover, under osmotic stress conditions, the membrane potential, calcium flux, and vacuolar pH changes in the *vsr1* mutant differ from those in the wild type. Given that manipulation of the intracellular pH is sufficient to modulate the expression of ABA biosynthesis genes, including *NCED3*, and ABA accumulation, we propose that intracellular pH changes caused by osmotic stress may play a signaling role in regulating ABA biosynthesis and that this regulation is dependent on functional VSR1.

Plant vacuoles are vital organelles for maintaining cell volume and cell turgor, regulating ion homeostasis and pH, disposing toxic materials, and storing and degrading unwanted proteins (Marty, 1999). To perform these diverse functions, vacuoles require an array of different and complex proteins. These proteins are synthesized at the endoplasmic reticulum (ER) and are transported to the vacuole through the vacuolar trafficking pathway. Perturbation of the vacuolar trafficking machinery affects many cellular processes, including tropisms, responses to pathogens, cytokinesis, hormone transport, and signal transduction (Surpin and Raikhel, 2004). The vacuolar trafficking system is comprised of several compartments: the ER, the Golgi apparatus, the trans-Golgi network (TGN), the prevacuolar compartment (PVC), and the vacuole. Vacuolar proteins synthesized at the ER are transported to the cis-Golgi via coat protein complex II (COPII) vesicles and are then transported to the TGN through the Golgi apparatus. In the TGN, proteins are sorted for delivery to their respective locations according to their targeting signal. Vacuolar proteins carrying a vacuolar sorting signal are thought to be recognized by vacuolar sorting receptors (VSRs), which are mainly located in the PVC, although sorting of vacuolar proteins may also occur at the ER and VSRs can be recycled from the TGN to the ER (Castelli and Vitale, 2005; Niemes et al., 2010). Multiple studies suggest that plant VSRs serve as sorting receptors both for lytic vacuole proteins (daSilva et al., 2005; Foresti et al., 2006; Kim et al., 2010) and for storage vacuole proteins (Shimada et al., 2003; Fuji et al., 2007; Zouhar et al., 2010).

Osmotic stress is commonly associated with many environmental stresses, including drought, cold, and high soil salinity, that have a severe impact on the productivity of agricultural plants worldwide. Therefore, understanding how plants perceive and respond to osmotic stress is critical for improving plant resistance to abiotic stresses (Zhu, 2002; Fujita et al., 2013). It has long been recognized that osmotic stress can activate several signaling pathways that lead to changes in gene expression and metabolism. One important regulator of these signaling pathways is the phytohormone abscisic acid (ABA), which accumulates in response to osmotic stress. ABA regulates many critical processes, such as seed dormancy, stomatal movement, and adaptation to environmental stress (Finkelstein and Gibson, 2002; Xiong and Zhu,

[1] This work was supported by the King Abdullah University of Science and Technology (to L.X.), the National Science Foundation (grant number IOS0919745 to J.Z.), and the National Institutes of Health (grant number R01GM059138 to J.-K.Z.).

* Address correspondence to liming.xiong@kaust.edu.sa.

The author responsible for distribution of materials integral to the findings presented in this article in accordance with the policy described in the Instructions for Authors (www.plantphysiol.org) is: Liming Xiong (liming.xiong@kaust.edu.sa).

[OPEN] Articles can be viewed without a subscription.
www.plantphysiol.org/cgi/doi/10.1104/pp.114.249268

  

2003; Cutler et al., 2010). De novo synthesis of ABA is of primary importance for increasing ABA levels in response to abiotic stress. ABA is synthesized through the cleavage of a C40 carotenoid originating from the 2-C-methyl-D-erythritol-4-phosphate pathway, followed by a conversion from zeaxanthin to violaxanthin catalyzed by the zeaxanthin epoxidase ABA1 and then to neoxanthin catalyzed by the neoxanthin synthase ABA4. Subsequently, a 9-cis-epoxycarotenoid dioxygenase (NCED) cleaves the violaxanthin and neoxanthin to xanthoxin. Xanthoxin, in turn, is oxidized by a short-chain alcohol dehydrogenase (ABA2) to abscisic aldehyde, which is converted to ABA by abscisic acid aldehyde oxidase3 (AAO3) using a molybdenum cofactor activated by the molybdenum cofactor sulfurase (ABA3; Nambara and Marion-Poll, 2005). In this pathway, it is generally thought that the cleavage step catalyzed by NCED is the rate-limiting step (Iuchi et al., 2000, 2001; Qin and Zeevaart, 2002; Xiong and Zhu, 2003). In Arabidopsis (*Arabidopsis thaliana*), five members of the NCED family (NCED2, NCED3, NCED5, NCED6, and NCED9) have been characterized (Tan et al., 2003). Of those, *NCED3* has been suggested to play a crucial role in ABA biosynthesis, and its expression is induced by dehydration and osmotic stress (Iuchi et al., 2000, 2001; Qin and Zeevaart, 2002; Xiong and Zhu, 2003). Thus, understanding how the *NCED3* gene is activated in response to osmotic stress is important for the elucidation of the mechanisms that govern plant acclimation to abiotic stress.

We have used the firefly luciferase reporter gene driven by the stress-responsive *NCED3* promoter to enable the genetic dissection of plant responses to osmotic stress (Wang et al., 2011). Here, we report the characterization of a unique regulator of ABA biosynthesis, 9-cis Epoxycarotenoid Dioxygenase Defective2 (CED2). The *ced2* mutants are impaired in osmotic stress tolerance and are defective in the expression of genes required for ABA synthesis and consequently osmotic stress-induced ABA accumulation. The *CED2* gene encodes VSR1, previously known to be involved in vacuolar trafficking but not known to be critical for osmotic stress induction of ABA biosynthesis and osmotic stress tolerance. Our study further suggests that intracellular pH changes might act as an early stress response signal triggering osmotic stress-activated ABA biosynthesis.

## RESULTS

### Identification and Characterization of the *ced2* Mutant

To understand the mechanisms of osmotic stress induction of ABA biosynthesis, we undertook a genetic approach to isolate Arabidopsis mutants with altered regulation of the *NCED3* gene by osmotic stress. A two-step screening was performed that involved imaging the *NCED3* promoter-driven firefly luciferase expression and measuring ABA levels as described previously (Wang et al., 2011). In this study, a new mutant, *ced2*, was identified as a unique regulator of ABA biosynthesis. ABA accumulation in the *ced2* mutant was reduced as compared with wild-type plants under the same osmotic stress generated by treating with polyethylene glycol (PEG; Fig. 1A). Because ABA levels are closely correlated with the transcript levels of genes required for ABA biosynthesis (Tan et al., 1997; Qin and Zeevaart, 1999; Thompson et al., 2000), we examined the transcript levels of ABA biosynthesis genes *ABA1*, *AAO3*, and *NCED3*. We found that the transcript levels of these genes were lower in the *ced2* mutant than in the wild-type plants under osmotic stress treatment (Fig. 1B). The *ced2* mutant is defective in osmotic stress-induced ABA accumulation that, in turn, is likely to negatively impact osmotic stress tolerance. In the presence of osmotic stress (on PEG-infused agar plates), germination and early seedling growth of the *ced2* mutant were markedly inhibited (Fig. 1, C and D; Supplemental Fig. S1, A and B). Moreover, the shoot and root growth was inhibited by osmotic stress treatments in both wild-type and *ced2* mutant seedlings, but the inhibition was more pronounced in the *ced2* mutant (Supplemental Fig. S1, C and D). These results indicate that *ced2* mutant plants are sensitive to osmotic stress during seed germination as well as during early seedling development.

Given that the *ced2* mutant was hypersensitive to osmotic stress, we then determined whether the mutant was also sensitive to salt stress. We compared seed germination and postgermination growth of the *ced2* mutant with wild-type plants but noted no significant difference between the mutant and wild-type plants at different salt concentrations (Supplemental Fig. S2, A–C). These results indicate that *ced2* mutant plants were not more sensitive to salt stress during seed germination and early seedling development.

We mapped the *ced2* mutation by crossing the *ced2* mutant with the Landsberg *erecta* ecotype to generate a F2 segregation population. F2 seedlings that showed increased osmotic stress sensitivity in shoots and roots on the PEG-infused agar medium were selected for molecular mapping. The *ced2* mutation was mapped to a 128-kb interval covered by bacterial artificial chromosome clones F8J2 and T4D2 on chromosome 3. We sequenced all of the open reading frames in this region in the *ced2* mutant and only found one mutation, a single nucleotide substitution from G to A at position 1,987 from the translation start site in the gene *At3g52850* (Fig. 2A). This mutation created a premature stop codon, resulting in the truncation of the encoded protein. The *At3g52850* gene was annotated as encoding VSR1, which binds vacuolar-targeting signals and sorts targeted proteins into vacuoles. To confirm that the mutation in *At3g52850* was responsible for the osmotic stress-sensitive phenotypes of the mutant, a genomic DNA fragment containing the entire *VSR1* gene (with about a 1.5-kb promoter region, the *VSR1* open reading frame, and 308 bp downstream of the stop codon) was transformed into the mutant. Twenty independent transgenic lines were obtained, and two $T_3$ lines were randomly chosen to test for osmotic stress sensitivity. The mutant seedlings remained hypersensitive to the osmotic stress treatment (–0.7 MPa PEG-infused agar plate), while the two transgenic lines no longer exhibited

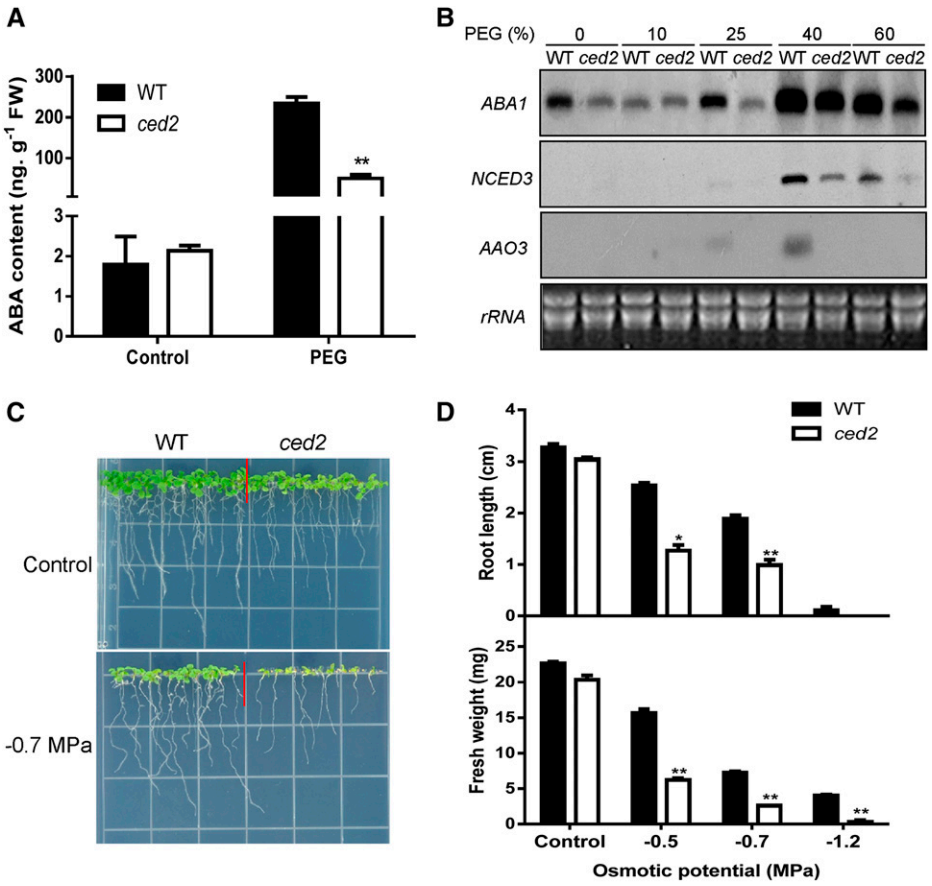


**Figure 1.** Isolation and characterization of the *ced2* mutant. A, ABA contents in *ced2* and wild-type (WT) seedlings under the control or osmotic stress treatment. Two-week-old seedlings were treated with 40% (w/v) PEG solution for 6 h before ABA measurement. FW, Fresh weight. B, RNA gel-blot analysis of the expression of ABA biosynthesis genes in *ced2* and wild-type plants in response to osmotic stress generated by the indicated concentrations of PEG. Ribosomal RNA (*rRNA*) was used as loading control. C, Morphology of seedlings on control or –0.7 MPa PEG-infused agar plates. Seeds were directly sowed on the shown plates, and pictures were taken 2 weeks after seed imbibition. D, Root growth (top) and shoot fresh weight (bottom) of wild-type and *ced2* seedlings on MS agar plates with different osmotic potentials at 2 weeks after seed imbibition. Six plants were pooled together for shoot fresh weight measurement per experiment. Three replicates were performed. Data in A and D represent means ± SE. $^{*}P < 0.05$ and $^{**}P < 0.01$.

these osmotic stress-sensitive phenotypes (Fig. 2B). These data demonstrated that *VSR1* could rescue the *ced2* mutant phenotypes and that *CED2* is the same gene as *VSR1*.

As the *ced2* mutant is a new allele of *VSR1*, we examined whether other *VSR1* alleles were also sensitive to osmotic stress. The *vsr1-2* allele had a transfer DNA (T-DNA) insertion in the seventh intron (Shimada et al., 2003), whereas *vsr1-3* and *vsr1-5* each had a single nucleotide substitution (Fuji et al., 2007). When grown on agar plates with –0.7 MPa of osmotic potential generated by PEG infusion, all mutants phenocopied the osmotic stress-sensitive phenotype of *ced2* (Fig. 2C), and serious damage was observed in the *vsr1-3* and *vsr1-5* mutants. To verify that the *ced2* mutant is allelic to other *vsr1* mutants, we performed genetic crosses among them. The resulting F1 seedlings were grown on –0.7 MPa PEG-infused agar plates, and the osmotic stress-sensitive phenotypes similar to those of the *ced2* or other *vsr1* mutants were observed among these F1 seedlings, indicating a lack of complementation among these mutant alleles (Fig. 2D). We also examined the expression of the *NCED3* gene in these *vsr1* mutants. Although these mutant alleles had slightly different expression levels of the gene, all showed lower induction of *NCED3* expression than the wild type in response to osmotic stress (Fig. 2E), demonstrating that *VSR1* is required for full induction of the *NCED3* gene in response to osmotic stress.

### Osmotic Stress-Regulated *VSR1* Expression Occurs via ABA-Dependent Pathways

We further investigated the expression of the *VSR1* gene in response to osmotic stress. The quantitative reverse transcription (qRT)-PCR analysis showed that the transcript level of *VSR1* was up-regulated within 6 h of osmotic stress treatment but returned to the control level after prolonged stress (Fig. 2F). We then asked whether the expression of *VSR1* is ABA dependent by performing qRT-PCR analysis of *VSR1* expression in two ABA-deficient mutants, *aba1-3* and *aba3-2*. Consistent with previous studies, the expression of *NCED3* was substantially lower in the *aba* mutants than in the wild-type plants under osmotic stress conditions. Interestingly, the expression of *VSR1* was also lower in the mutants, which suggested that *VSR1* is at least partly regulated via ABA-dependent pathways (Supplemental Fig. S3).

### The *ced2* Mutant Is Sensitive to ABA and Accumulates More ROS

We determined whether the *ced2* mutant is also sensitive to ABA. The seed germination and seedling greening rates were significantly lower than those of the wild type in the presence of 0.1 to 0.5 $\mu$M ABA (Fig. 3, A and B). We then tested whether postgermination growth was affected

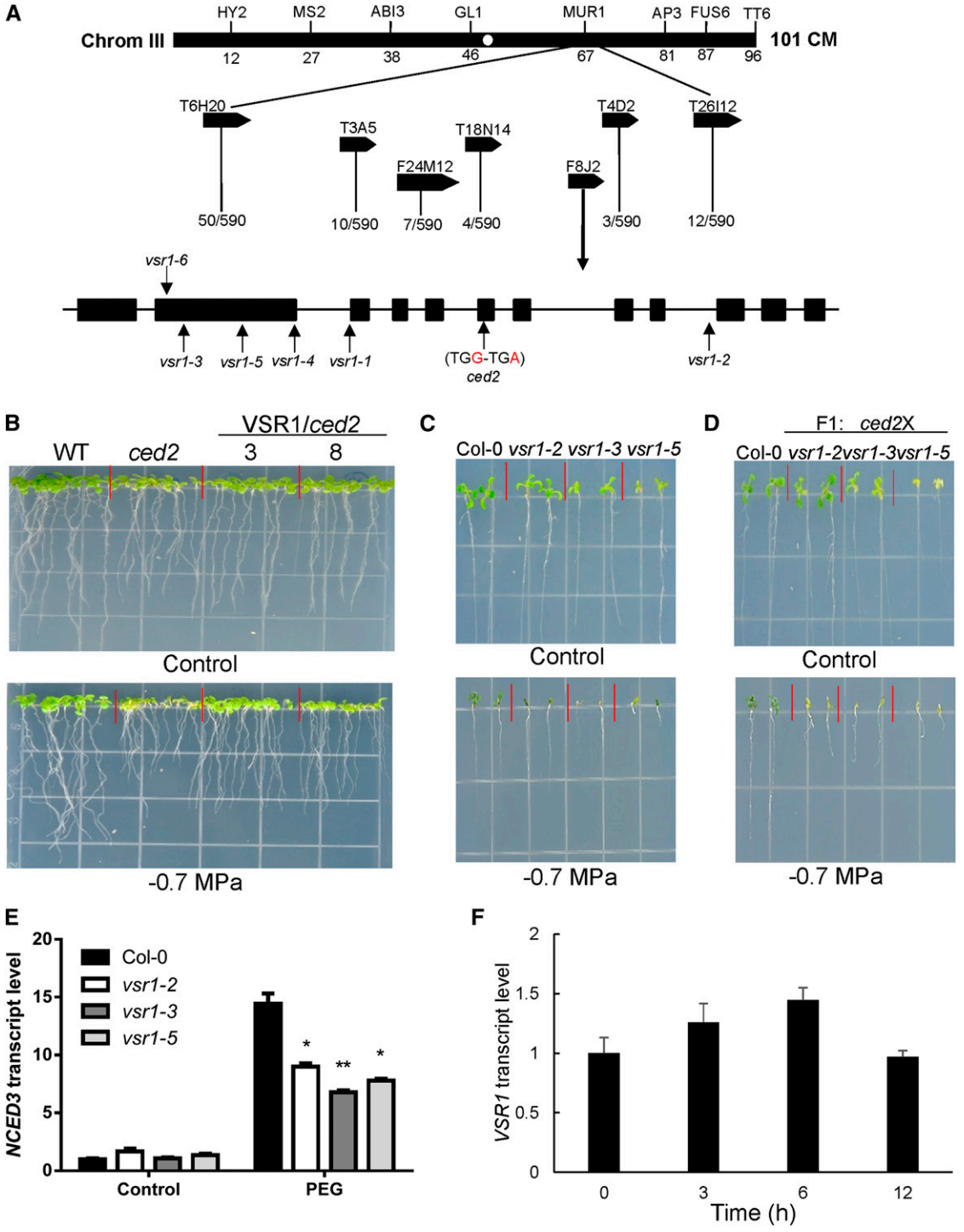


**Figure 2.** Map-based cloning and complementation of the *ced2* mutation and the expression of *VSR1* under osmotic stress treatments. A, By analyzing 590 recombinant chromosomes, the *CED2* locus was mapped to the lower arm of chromosome 3 between the bacterial artificial chromosome clones F8J2 and T4D2. DNA sequencing revealed that the *ced2* mutant had a point mutation in the sixth exon of the At3g52850 gene. Positions of mutations in each allele are indicated by vertical arrows. B, Complementation of *ced2* by the wild-type *CED2*/*VSR1* gene. The wild type (WT), *ced2*, and two homozygous *ced2* transgenic lines (nos. 3 and 8) expressing the wild-type *CED2* gene are shown. Plants were grown on MS (Control, top) or –0.7 MPa PEG-infused agar plates (bottom). The photographs were taken 10 d after seed imbibition. C, *vsr1* mutant alleles were sensitive to osmotic stress. Seeds were germinated, and seedlings were grown on control (top) or –0.7 MPa PEG-infused MS agar plate (bottom) for 2 weeks before taking the pictures. D, The *ced2* mutant is a new allele of VSR1. Wild-type and F1 plants (*ced2*/*vsr1-2*, *ced2*/*vsr1-3*, and *ced2*/*vsr1-5*) were grown on MS (Control, top) or –0.7 MPa PEG-infused agar plate (bottom) for 2 weeks before

by the *ced2* mutation under ABA treatment. Root and shoot growth was inhibited by ABA treatments in both wild-type and *ced2* mutant seedlings, but the inhibition was more pronounced in the *ced2* mutant (Fig. 3, C and D). These results are consistent with previous observations that ABA-deficient mutants tend to be sensitized to ABA in physiological and molecular responses, presumably to compensate for their lower internal ABA levels (Xiong et al., 2001a, 2001b, 2002).

Reactive oxygen species (ROS) have been implicated as second messengers in osmotic stress and ABA-mediated cellular responses in plants. ROS signal can be perceived and transduced to activate redox-related proteins, which, in turn, mediate the induction of gene expression (Mustilli et al., 2002; Fujita et al., 2013). Nonetheless, the accumulation of ROS can also cause cellular damage. ROS were visualized by staining with 2′,7′-dichlorofluorescein diacetate ($H_2$DCF-DA) following the treatment of 40% (w/v) PEG or 50 $\mu$M ABA for 3 h. In the root tip region, the *ced2* mutant accumulated more ROS than did the wild-type plants under the control conditions (Fig. 3, E and F). After a 3-h exposure to a medium containing either 40% (w/v) PEG or 50 $\mu$M ABA, the ROS contents increased in both the *ced2* mutant and wild-type plants. However, the *ced2* mutant accumulated more ROS than did the wild type in response to ABA treatment. Under the osmotic stress treatment, ROS levels in the wild type and the *ced2* mutant, although they increased, were at a similar magnitude compared with control conditions (Fig. 3, E and F).

### The *ced2* Mutant Is Defective in the Positive Feedback Regulation of ABA Biosynthesis Genes by ABA and Is Drought Sensitive

While studying the ABA biosynthesis genes *ABA3/LOW EXPRESSION OF OSMOTIC STRESS GENE5* (*LOS5*; Xiong et al., 2001b) and *ABA1/LOS6* (Xiong et al., 2002), it was found that ABA positively feedback regulates the expression of several ABA biosynthesis genes. This autoregulation of ABA biosynthesis genes is impaired in *supersensitive to ABA and drought1* (*sad1*), a mutant defective in drought-induced ABA biosynthesis that is also sensitive to ABA (Xiong et al., 2001a). Because *ced2* mutant is sensitive to ABA and defective in the expression of ABA biosynthesis genes in response to PEG-induced osmotic stress, it is conceivable that CED2 may be involved in the autoregulation of ABA biosynthesis genes by ABA. To test this hypothesis, we examined the transcript levels of ABA biosynthesis genes *ABA1*, *NCED3*, and *AAO3* in response to ABA treatments and noted that the transcript levels of these genes increased in response to exogenous ABA in wild-type plants, and while an increase was also seen in the *ced2* mutant, it remained lower (Fig. 3G). As a control, the induction of these ABA biosynthesis genes under PEG-induced osmotic stress treatment was significantly lower in the *ced2* mutant when compared with wild-type plants (Fig. 3G). These data suggest that the *ced2* mutant is impaired in the positive feedback regulation of ABA biosynthesis genes.

Plant drought tolerance is tuned by a complex molecular and cellular network that closely interacts with ABA signaling pathways. In ABA-hypersensitive mutants, such as *enhanced response to ABA1* (Cutler et al., 1996), *ABA hypersensitive1* (Hugouvieux et al., 2001), and *ABA-overly sensitive1* (*abo1*; Chen et al., 2006), increased ABA sensitivity is accompanied by reduced transpiration water loss and increased drought tolerance. By contrast, *sad1* (Xiong et al., 2001a) and *abo3* (Ren et al., 2010) mutants show sensitivity to ABA and increased transpiration water loss. Because the *ced2* mutant is defective in osmotic stress tolerance and is sensitive to ABA during seed germination and seedling growth, we tested it for drought tolerance. We first measured transpiration water loss rates in detached leaves and found that the *ced2* mutant leaves lost water much faster than did the wild-type leaves (Supplemental Fig. S4A), with a water loss rate similar to that of the *sucrose nonfermenting1 related kinase2.6/open stomata1* mutant (Mustilli et al., 2002; Yoshida et al., 2002; Fujii et al., 2007), consistent with defective stomatal regulation in the *ced2* mutant. To determine whether this defect was caused by ABA deficiency or ABA insensitivity, exogenous ABA was applied to the mutant and wild-type plants. Treatment with ABA reduced the rate of water loss in the *ced2* mutant and wild-type plants to a similar degree (Fig. 3H), therefore implying that exogenous ABA could partially rescue the increased water loss phenotype caused by impaired drought-induced ABA biosynthesis in the *ced2* mutant. Further examination showed that the *ced2* mutant was less responsive to ABA in closing stomata (Fig. 3, I and J). We also analyzed ABA levels in the *ced2* mutant under drought stress. The stress treatment increased ABA content in the wild-type plants but not in the *ced2* mutant, indicating that drought-induced ABA biosynthesis was impaired (Fig. 3K). It is therefore likely that the increased transpiration rate of the *ced2* mutant leaves may cause the effect on drought resistance. However, the *ced2* mutant is smaller than the wild-type plants when grown in soil, and therefore the reduced total leaf surface area may have contributed to the reduced overall transpiration, thereby masking differences in drought resistance between

**Figure 2**. (*Continued.*)
taking the pictures. E, Transcript levels of *NCED3* in the wild type and three *vsr1* mutant alleles under the control or 40% (w/v) PEG treatment for 6 h. F, Regulation of *CED2/VSR1* expression by osmotic stress. RNA was extracted from 2-week-old wild-type ecotype Columbia (Col-0) plants treated with 40% (w/v) PEG solution for the indicated time and was used for qRT-PCR analysis. In E and F, real-time reverse transcription-PCR quantifications were normalized to the expression of *Polyubiquitin3* (*UBQ3*). Error bars represent SE from three biological replicates. $*P < 0.05$ and $**P < 0.01$.

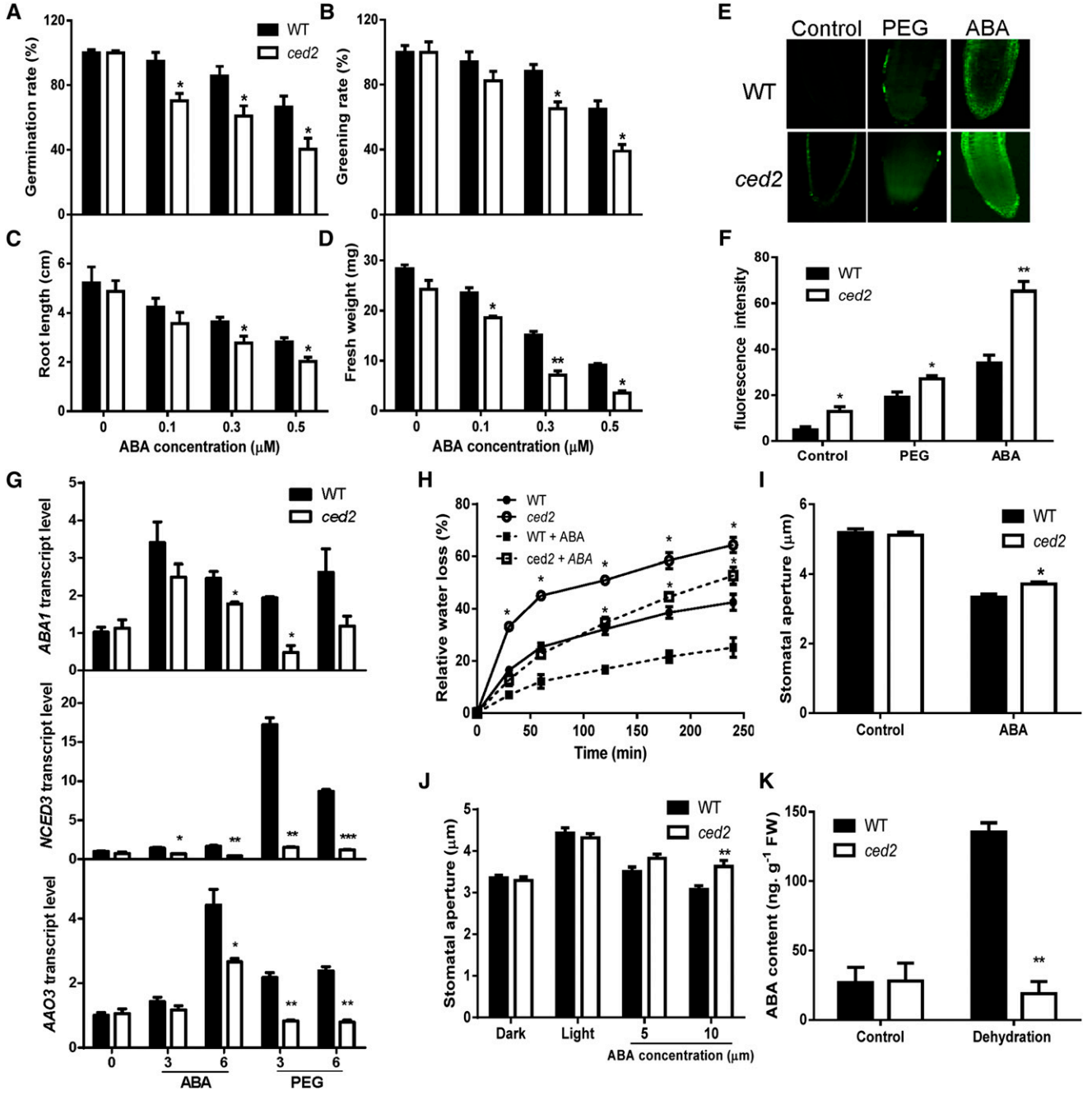


**Figure 3.** Stress and ABA responses in the *ced2* mutant. A, Seed germination rate on MS agar plates supplemented with different concentrations of ABA at 4 d after seed imbibition. Four replicates were performed with about 100 seeds per genotype for each replicate. B, Greening rate of seedlings on ABA-supplemented MS agar plates at 8 d after seed imbibition. Four replicates were performed. C, Fresh weight of seedlings on ABA-supplemented MS agar plates at 2 weeks after seed imbibition. Six plants were pooled together for weight measurement per replicate. Three replicates were performed. D, Root growth of seedlings on ABA-supplemented MS agar plates at 2 weeks after seed imbibition. Three replicates were performed. E, Representative images of ROS production stained with the fluorescent dye $H_2$DCF-DA in root tips under the control (left), PEG (middle), and ABA treatment (right). F, Quantification of relative ROS production based on fluorescence pixel intensity. Three replicates were performed with 10 seedlings for each genotype per replicate. G, qRT-PCR analysis of transcript levels of *ABA1*, *NCED3*, and *AAO3* in seedlings under ABA and PEG treatments. Real-time reverse transcription-PCR quantifications were normalized to the expression of *UBQ3*. The transcript level in Col-0 under the control conditions was set to 1.0. H, Transpirational water loss of detached leaves. Soil-grown plants were sprayed with water or 50 $\mu$M ABA, and leaves were detached 4 h later for measuring water loss at the indicated time. I, Stomatal aperture at 2.5 h after 10 $\mu$M ABA treatment. J, Inhibition of light-induced stomatal opening by ABA. K, ABA content of *ced2* and wild-type seedlings after dehydration treatment for 2 h. Three replicates were performed. Black bars indicate the wild type (WT), and white bars indicate *ced2* mutant. In I and J, at least 120 stomata were analyzed. Data in A to D and F to K represent means ± SE. $*P < 0.05$ and $**P < 0.01$.

the *ced2* mutant and wild-type plants (Supplemental Fig. S4, B and C). To more reliably assess the drought sensitivity of the *ced2* mutant plants irrespective of the size of the plants, we employed electrolyte leakage as an indicator of drought-induced cellular damage. The *ced2* mutant seedlings had a similar electrolyte leakage rate as that of the wild-type plants without PEG treatment. While in the presence of 40% (w/v) PEG, the *ced2* mutant seedlings showed greater electrolyte leakage (Supplemental Fig. S4D), indicating that the integrity of the *ced2* mutant plasma membrane was more severely compromised by drought stress.

### Transcriptome Analysis of the *ced2* Mutant in Response to Osmotic Stress

To further examine the role of the *ced2* mutant in global gene regulation, we performed microarray experiments using Agilent Arabidopsis ATH1 gene expression arrays to compare the transcriptome of the mutant with that of the wild type under osmotic stress conditions. As compared with the wild type, osmotic stress increased the expression of 1,849 genes and decreased that of 710 genes in the mutant (Fig. 4A; Supplemental Table S1). To categorize the genes with altered expression in the *ced2* mutant in response to osmotic stress, we performed Gene Ontology (http://www.arabidopsis.org/tools/bulk/go) and Go Term Enrichment (http://amigo.geneontology.org/cgi-bin/amigo/term_enrichment) analyses with manual adjustment when necessary (Supplemental Fig. S5, A and B). Interestingly, in the group of down-regulated genes, we observed an enrichment of genes related to water stimulus in the biological process (Supplemental Table S2). We then analyzed the expression patterns of the top 400 genes that were up- or down-regulated in the *ced2* mutant by using the Genevestigator tool (Hruz et al., 2008). A large number of genes that showed lower expression levels in the mutant under osmotic stress in our ATH1 array experiments are up-regulated by ABA and osmotic stress, while the highly expressed genes in the *ced2* mutant are mostly repressed by such stimuli (Fig. 4B). These data are consistent with the interpretation that VSR1 regulates the expression of osmotic stress- and/or ABA-responsive genes, including ABA biosynthesis genes under osmotic stress conditions. To ascertain the validity of the microarray data, we selected 12 genes related to dehydration stress that

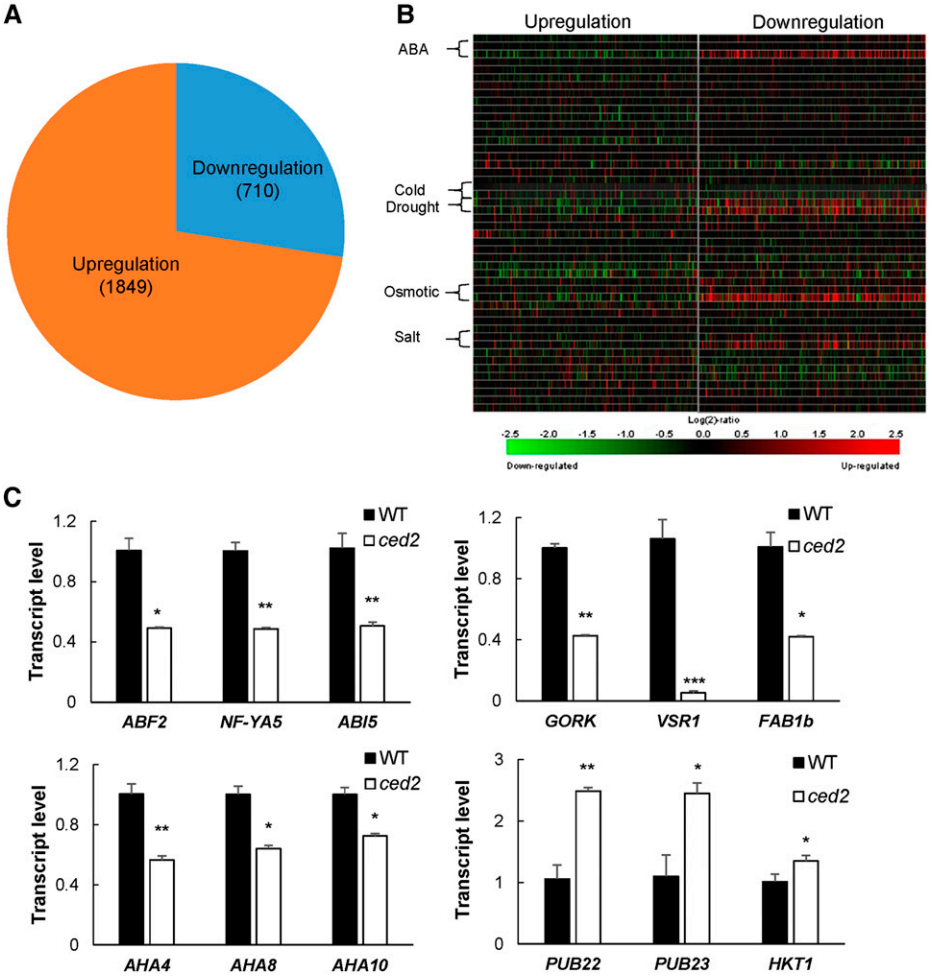


**Figure 4.** Transcriptome analysis of the *ced2* mutant under osmotic stress. A, Number of genes with altered expression in the *ced2* mutant relative to the wild-type plants. Two-week-old plants were treated with 40% (w/v) PEG solution for 6 h. RNAs from two biological repeats were extracted for microarray analysis. B, Heat maps indicating stimulus responsiveness of the top 400 genes in the up-regulated or down-regulated group from microarray analysis as shown in A. The heat maps were generated from Genevestigator stimulus data sets. C, Confirmation by real-time reverse transcription-PCR quantifications of the expression of stress-related genes with significant changes in expression levels between the wild type (WT) and *ced2* mutants from the microarray analysis. Total RNA was extracted from *ced2* and wild-type plants under osmotic stress treatment (40% [w/v] PEG, 6 h). The expression of individual genes was normalized to that of *UBQ3*. The transcript level in the wild type was set to 1.0. Error bars represent SE from three replicates. $*P < 0.05$, $**P < 0.01$, and $***P < 0.001$.

showed significant up- or down-regulation in the microarray assays to examine their expression levels by qRT-PCR. In agreement with the microarray results, *ABSCISIC ACID RESPONSIVE ELEMENT-BINDING FACTOR2* (AT1G45249), *NUCLEAR FACTOR Y SUBUNIT A5* (AT1G54160), *ABSCISIC ACID INSENSITIVE5* (AT2G36270), *GATED OUTWARDLY-RECTIFYING $K^+$ CHANNEL* (AT5G37500), *VSR1* (AT3G52850), *FORMS APLOID AND BINUCLEATE CELLS 1B* (AT3G14270), *$H^+$-ATPASE4* (*AHA4*; AT3G47950), *AHA8* (AT3G42640), and *AHA10* (AT1G17260) showed lower expression levels, while *PLANT U-BOX22* (*PUB22*; AT3G52450), *PUB23* (AT2G35930), and *HIGH-AFFINITY $K^+$ TRANSPORTER1* (AT4G10310) showed higher expression levels in the *ced2* mutant compared with wild-type plants (Fig. 4C). These results indicate that the *ced2* mutant is impaired in osmotic stress regulation of a large number of genes.

### Role of VSR-Mediated Vacuolar Trafficking in Osmotic Stress Regulation of ABA Biosynthesis and Osmotic Stress Tolerance

Given that homomeric interaction of the VSR1 protein through the transmembrane domain and C-terminal cytoplasmic domain is essential for vacuolar trafficking of soluble proteins and that two dominant-negative mutations (*C2A*:HA 4-3 and *C2A*:HA 7-6) with Ala substitution interfered with the homomeric interaction and inhibited vacuolar trafficking (Kim et al., 2010), we first examined the osmotic stress sensitivity in transgenic plants expressing these two dominant-negative mutations along with one overexpressing the wild-type *VSR1* (*VSR1*:HA). Despite the slight difference in their sensitivity to osmotic stress between the two transgenic lines that may have been caused by their different mechanism of inhibition of vacuolar trafficking, germination and seedling growth of the dominant-negative mutants were more inhibited by the stress than those of the wild type (Fig. 5A). On the other hand, overexpression of wild-type *VSR1*:HA did not affect osmotic stress tolerance compared with the wild-type plants, consistent with the fact that these overexpressors did not inhibit vacuolar trafficking (Kim et al., 2010). These two dominant-negative mutant lines also had lower levels of ABA biosynthesis gene transcripts compared with the wild type and the *VSR1*-overexpressing line (Fig. 5, B and C). These data suggest that vacuolar trafficking mediated by VSR1 is important for osmotic stress-regulated ABA biosynthesis and, consequently, osmotic stress tolerance.

In Arabidopsis, the VSR family has seven members, *VSR1* to *VSR7*. We examined whether other VSRs are also involved in osmotic stress-induced ABA biosynthesis and osmotic stress tolerance and found that, except for *vsr3*, none of these single mutants showed any obvious difference in seed germination (Supplemental Fig. S6, A and B) or in the expression of *NCED3* under osmotic stress conditions relative to the wild type (Supplemental Fig. S6C). Given that recent studies showed *VSR1*, *VSR3*, and *VSR4* are involved in lytic and protein storage vacuole trafficking pathways (Zouhar et al., 2010; Lee et al., 2013) and whereas *VSR5*, *VSR6*, and *VSR7* may be involved in sorting salicylic acid-induced or Nonexpresser of pathogenesis-related genes1-dependent pathogenesis-related vacuolar proteins (Wang et al., 2005), we examined whether there is functional redundancy in VSRs in osmotic stress induction of ABA biosynthesis and osmotic stress tolerance. The results demonstrated that *vsr1/vsr3* and *vsr1/vsr4* double mutants showed obvious inhibition during germination and postgermination growth on the PEG-infused agar plates relative to the wild type (Fig. 5, D and E), whereas *vsr5/vsr6* did not (Supplemental Fig. S6B). Furthermore, ABA biosynthesis gene expression was also lower in *vsr1/vsr3* and *vsr1/vsr4* than in the wild type (Fig. 5F).

### Osmotic Stress Differentially Affects Membrane Depolarization, Calcium Flux, and Vacuolar Alkalization in *vsr* Mutants

Our studies uncovered an unexpected link between vacuolar trafficking and ABA biosynthesis, as well as stress signaling. Based on previous reports that membrane potentials of the vacuole and plasma membrane rapidly respond to osmotic stress prior to changes in gene expression (Lew, 2004), we determined the effect of osmotic stress on membrane potentials in planta using the fluorescent dye bis-(1,3-dibarbituric acid)-trimethine oxanol (Konrad and Hedrich, 2008; Supplemental Fig. S7A). PEG-induced osmotic stress caused a transient increase in membrane depolarization both in the wild-type and mutant plants. However, the depolarization was significantly higher in the *ced2*, *vsr1/vsr3*, and *vsr1/vsr4* mutants than in the wild-type plants, as shown by increased voltage-sensitive fluorescence in the mutants (Fig. 6, A and B), although membrane potentials restored to near basal levels both in the wild type and mutants under prolonged PEG treatment.

Because osmotic stress triggers rapid transient changes in the second messengers, such as $Ca^{2+}$, which then activate or modulate downstream signaling (Dodd et al., 2010), we studied changes in cytosolic calcium ($[Ca^{2+}]_{cyt}$) in response to osmotic stress using the fluorescent dye Fluo-4 acetoxymethyl (AM) ester. In nonstressed seedlings, no significant difference was observed in $[Ca^{2+}]_{cyt}$ in the root tips and root elongation zone between the wild type and the mutant (Fig. 6, C and D). However, in response to osmotic stress, $[Ca^{2+}]_{cyt}$ markedly increased in the *ced2*, *vsr1/vsr3*, and *vsr1/vsr4* mutants compared with those in the wild-type plants or in the *vsr5/vsr6* double mutant (Fig. 6, C and D; Supplemental Fig. S7B).

In plant cells, cation/$H^+$ antiporters in the Golgi, TGN, endosome, and PVC contribute to the regulation of the cation concentration as well as the pH in these compartments and thereby affect vesicle trafficking (Nakamura et al., 2005; Pardo et al., 2006; Krebs et al., 2010; Bassil et al., 2011). The sustained level of intracellular $Ca^{2+}$ is diagnostic for an effect on one or several $Ca^{2+}$ transporters, such as cation exchangers (Sze et al., 2000). Because these

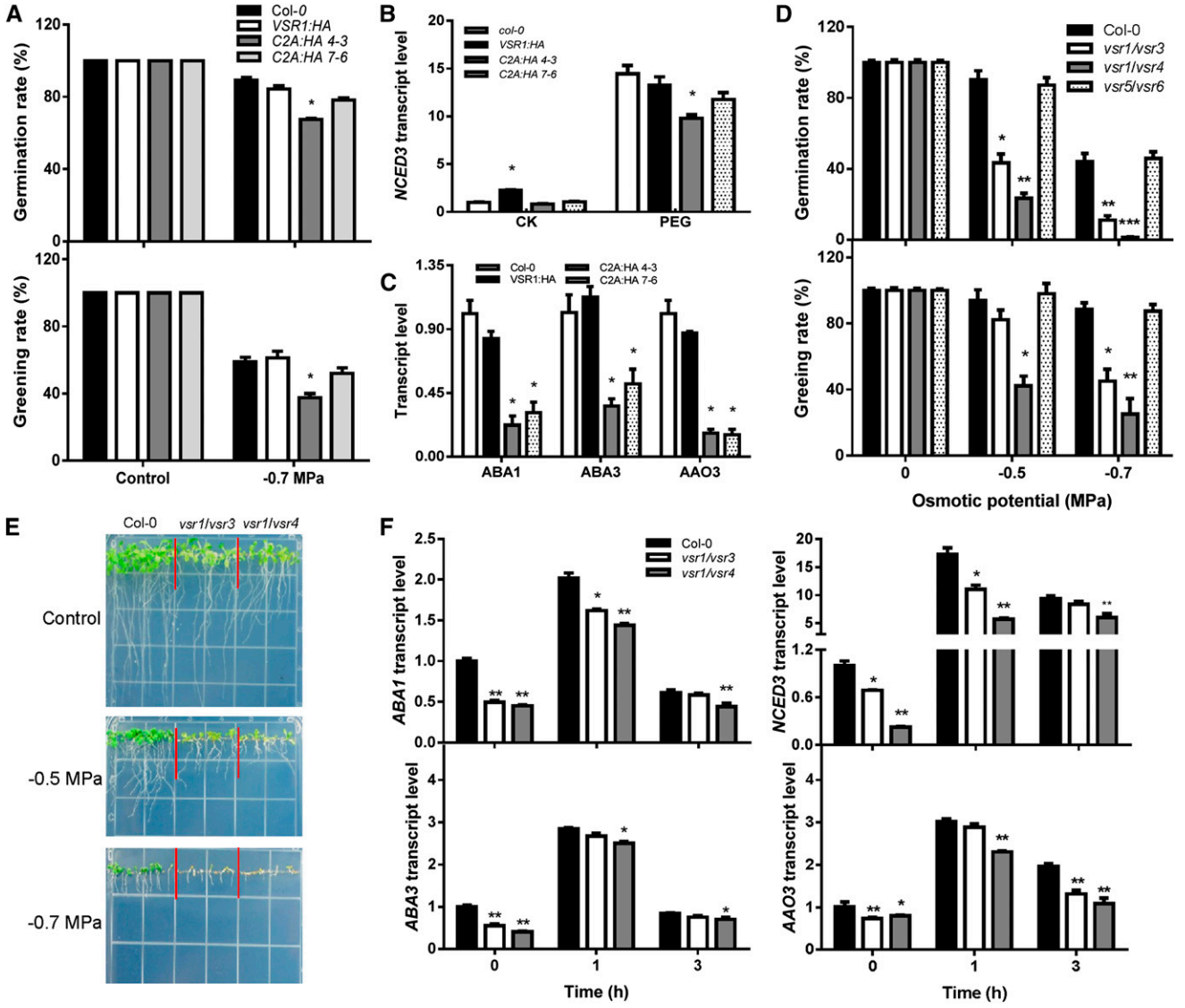


**Figure 5.** Vacuolar trafficking mediated by VSRs is required for osmotic stress regulation of ABA biosynthesis and stress tolerance. A, Seed germination and seedling greening rates on the control or PEG-infused agar plates (–0.7 MPa). Four replicates were performed. B, Transcript levels of *NCED3* in seedlings under the control (CK) or osmotic stress treatment (40% [w/v] PEG). C, Transcript levels of ABA biosynthesis genes in seedlings under 40% (w/v) PEG treatment. D, Seed germination and seedling greening rates on the control or PEG-infused agar plates. Four replicates were performed. E, Morphology of Col-0 and *vsr* double mutants on the control or PEG-infused agar plates. Seeds were directly sowed on the shown plates, and pictures were taken 10 d after sowing. F, Transcript levels of ABA biosynthesis genes in seedlings in response to PEG treatment. Col-0 indicates the wild type; VSR1:HA indicates transgenic plants overexpressing *VSR1*; C2A:HA 4-3 and C2A:HA 7-6 indicate two independent transgenic lines expressing the dominant-negative form of VSR1 (C2A); and *vsr1/vsr3*, *vsr1/vsr4*, and *vsr5/vsr6* indicate double mutants. Data in A to D and F represent means ± SE. $*P < 0.05$, $**P < 0.01$, and $***P < 0.001$. For qRT-PCR analysis (B, C, and F), real-time reverse transcription-PCR quantifications were normalized to the expression of *UBQ3*. The transcript level in Col-0 under the control conditions was set to 1.0.

exchangers are energized by the proton gradient between the vacuole and the cytoplasm, we investigated whether *ced2/vsr1* mutants showed differences in the pH gradients between the compartments that might explain the differences in the $Ca^{2+}$ signature. To do this, we used the ratiometric fluorescein-based, pH-sensitive dye 2′,7′-bis-(2-carboxyethyl)-5-(and-6)-carboxyfluorescein (BCECF) with membrane-permeable AM ester that was readily loaded into the vacuoles of intact roots (Supplemental Fig. S7C). In situ calibration curves were established by determining the fluorescence ratios of confocal images in different pH values of the equilibration buffers (Supplemental Fig. S7D). It was observed that vacuolar pH ($pH_{vac}$) in cells at the root tip was lower

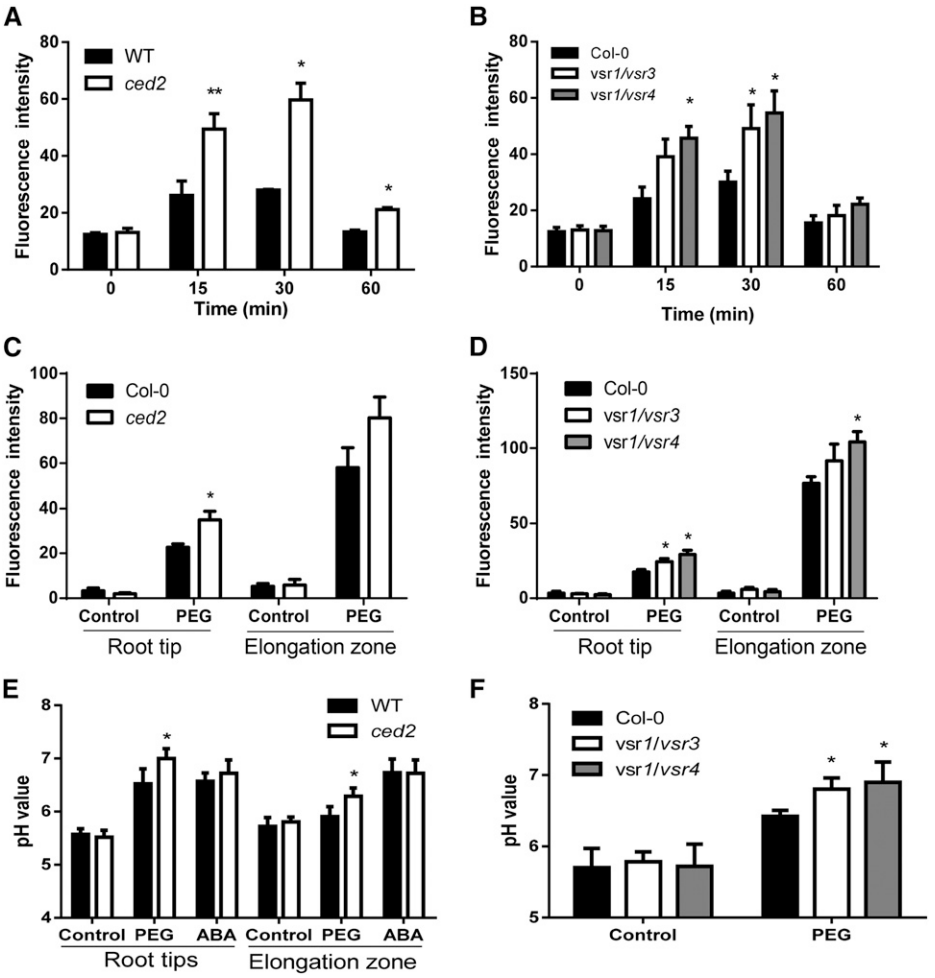


**Figure 6.** VSRs maintained membrane potential, calcium flux, and $pH_{vac}$ under osmotic stress. A, Time course of the relative membrane potential in roots of the wild type (WT) and *ced2* in response to 40% (w/v) PEG treatment. B, Time course of the relative membrane potential in roots of the Col-0, *vsr1/vsr3*, and *vsr1/vsr4* in response to 40% (w/v) PEG treatment. C, Calcium flux in roots of the wild type and *ced2* in response to 40% (w/v) PEG treatment. D, Calcium flux in roots of the Col-0, *vsr1/vsr3*, and *vsr1/vsr4* in response to 40% (w/v) PEG treatment. E, $pH_{vac}$ in root tips and mature roots of the wild type and *ced2* with or without 40% (w/v) PEG treatment for 1 h. F, $pH_{vac}$ in roots of the Col-0, *vsr1/vsr3*, and *vsr1/vsr4* in response to 40% (w/v) PEG treatment. For membrane potential and calcium flux assays, three independent experiments with 10 seedlings each were performed for each genotype. For $pH_{vac}$ measurements, three independent experiments were performed with 15 seedlings for each genotype. Data in A to F represent means ± SE. $^*P < 0.05$ and $^{**}P < 0.01$. Col-0 indicates the wild type; *ced2* indicates *ced2* mutant; *vsr1/vsr3* and *vsr1/vsr4* indicate double mutants.

(pH 5.5) than in the mature zone (pH 5.7; Fig. 6E), and this is consistent with a previous study (Bassil et al., 2011). Under the control conditions, no significant difference in $pH_{vac}$ occurred in the root elongation zone between the wild type and the *vsr* mutants (Fig. 6, E and F). By contrast, the $pH_{vac}$ in cells in the elongation zone of *ced2*, *vsr1/vsr3*, and *vsr1/vsr4* mutants was higher than that in the wild-type plants in response to PEG treatment (Fig. 6, E and F), whereas the $pH_{vac}$ of the *vsr5/vsr6* mutant did not differ from that in the wild type (Supplemental Fig. S7E).

### The Intracellular pH Homeostasis as a Signal in the Regulation of Osmotic Stress-Induced ABA Biosynthesis

The changes in intracellular pH homeostasis in *vsr* mutants in response to osmotic stress prompted us to investigate whether $pH_{vac}$ does directly affect the regulation of ABA biosynthesis in response to osmotic stress. Using a specific inhibitor of vacuolar-type $H^+$-adenosine triphosphatase (V-ATPase), concanamycin A (ConcA), to raise the $pH_{vac}$ (Krebs et al., 2010), we determined the transcript levels of ABA biosynthesis genes under the control and PEG treatment. The transcript level of *NCED3* increased in seedlings treated with ConcA (500 nM) under the control conditions. However, under osmotic stress, the transcript level of *NCED3* was significantly decreased in ConcA-treated seedlings, while the transcript level of *ABA1* did not show obvious change either with or without osmotic stress treatment (Fig. 7A).

Because it is known that V-ATPase maintains the acidic pH of the endomembrane system (Herman et al., 1994; Dettmer et al., 2006), we determined whether the inhibition of the primary $H^+$ pumps has an effect on the regulation of ABA biosynthesis. We first determined whether the transcript level of ABA biosynthesis genes was altered in the *vacuolar $H^+$ ATPase A2* (*vha-a2*)/*vha-a3* double mutant that lacks both subunits A of the tonoplast V-ATPase (Krebs et al., 2010). Surprisingly, we did not observe significant change in the expression level of the ABA biosynthesis genes under control or osmotic stress (Fig. 7B). Because previous studies showed that the *de-etiolated3* (*det3*) mutant has a reduced V-ATPase activity (Schumacher et al., 1999) and increased alkalization of the endosomal system (Brüx et al., 2008), we tested whether this mutant is affected in ABA biosynthesis.

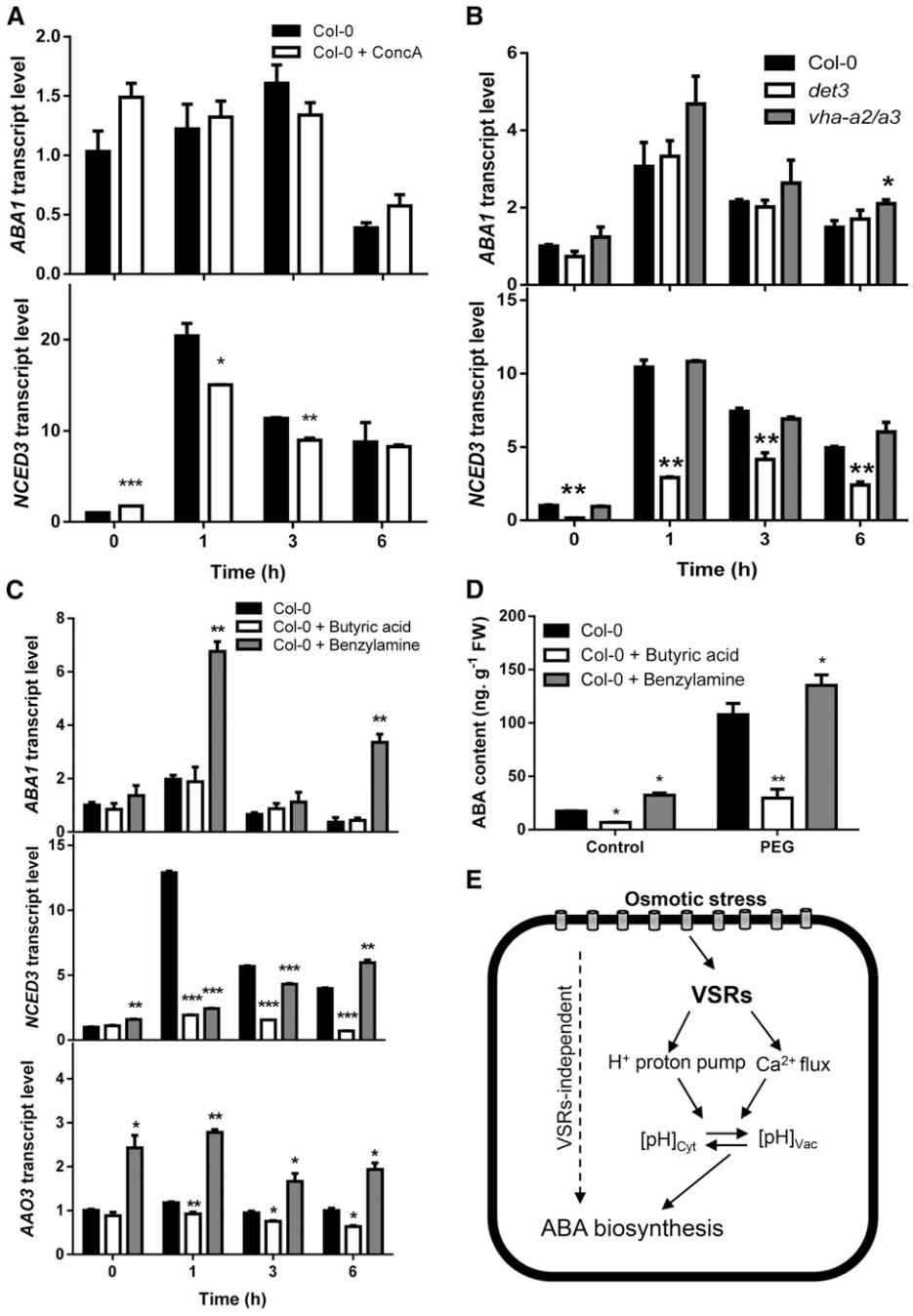


**Figure 7.** ABA biosynthesis regulated by intracellular pH homeostasis. A, Transcript levels of ABA biosynthesis genes *ABA1* (top) and *NCED3* (bottom) in Col-0 under osmotic stress (40% [w/v] PEG) with or without ConcA pretreatment. B, Transcript levels of ABA biosynthesis genes *ABA1* (top) and *NCED3* (bottom) in Col-0, *vha-a2/vha-a3*, and *det3* under 40% (w/v) PEG treatment. C, Transcript levels of ABA biosynthesis genes *ABA1* (top), *NCED3* (middle), and *AAO3* (bottom) in Col-0 under osmotic stress (40% [w/v] PEG) with or without 10 mM butyric acid or 10 mM benzylamine pretreatment. D, ABA content in Col-0 under osmotic stress (40% [w/v] PEG) with or without 10 mM butyric acid or 10 mM benzylamine pretreatment. Three replicates were performed. E, A model proposing the function of VSRs in regulating ABA biosynthesis and ABA signaling. Upon encountering osmotic stress, an osmosensor perceives the signal and leads to changes in cell turgor and cell volume, which are maintained by the vacuole. Osmotic stress also activates an undefined upstream signaling pathway that triggers ABA biosynthesis as well as downstream ABA signal transduction. VSRs function in sorting soluble lytic vacuole proteins or vacuole storage proteins that might affect the activity of proton pumps or ions channels, which, in turn, maintain the pH homeostasis between the cytoplasm and the vacuole. Intracellular pH homeostasis could act as a signal to activate ABA biosynthesis and signaling. A hypothetical VSR1-independent regulation of ABA biosynthesis (dashed line) is also shown. In A to C, real-time reverse transcription-PCR quantifications were normalized to the expression of *UBQ3*. The transcript level in Col-0 under control conditions was set to 1.0. Data in A to D represent means ± SE. $^{*}P < 0.05$, $^{**}P < 0.01$, and $^{***}P < 0.001$. FW, Fresh weight.

The transcript level of *NCED3* was significantly decreased in *det3* mutants compared with wild-type plants, although the transcript level of *ABA1* did not show obvious change (Fig. 7B). Moreover, osmotic stress-activated ABA accumulation in *det3* mutants was also lower compared with wild-type plants, while *vha-a2/vha-a3* was not (Supplemental Fig. S8). Taken together, these results suggest that osmotic stress-induced ABA biosynthesis is dependent on the pH of the endosomal system that, in turn, is maintained by the activity of the V-ATPase.

In the next series of experiments, we investigated whether the changes in the cytosolic pH ($pH_{cyt}$) are sufficient to regulate ABA biosynthesis in response to osmotic stress. We pretreated the tissue with butyric acid, a weak cell-permeable acid, to induce cytosolic acidification (Bibikova et al., 1998) and benzylamine, a weak cell-permeable base, to induce cytosolic alkalization (Romani et al., 1998; Zhang et al., 2001) before imposing osmotic stress and then examined their effects on transcript levels of ABA biosynthesis genes. When wild-type Col-0 plants were pretreated with 10 mM

butyric acid or 10 mM benzylamine for 1 h and briefly rinsed before being subjected to 40% (w/v) PEG treatment, the transcript levels of *ABA1*, *NCED3*, and *AAO3* could still be induced by osmotic stress in the wild-type plants. However, the transcript levels of these genes were significantly reduced in butyric acid-pretreated plants but increased in benzylamine-pretreated plants under osmotic stress (Fig. 7C). We next determined whether ABA accumulation was affected by the pH change-inducing pretreatments in the wild type under osmotic stress conditions and found that osmotic stress-induced ABA accumulation was greatly reduced in wild-type plants following cytosolic acidification and increased as a result of cytosolic alkalization (Fig. 7D). These results are therefore consistent with a key role of intracellular pH homeostasis in the regulation of osmotic stress-induced expression of ABA biosynthesis genes as well as ABA biosynthesis in general (Fig. 7E).

## DISCUSSION

In this study, we identified CED2/VSR1 as a unique component essential for osmotic stress-regulated ABA biosynthesis and osmotic stress resistance. The *ced2/vsr1* mutants are also impaired in ABA response and the positive regulation of ABA biosynthesis genes by ABA (Fig. 3). This regulation is important for ABA biosynthesis and drought resistance, as the *sad1* mutant defected in this regulation also exhibited increased drought stress sensitivity (Xiong et al., 2001b). The role of VSR1 in vacuolar trafficking has been well established (daSilva et al., 2005; Foresti et al., 2010; Kim et al., 2010), yet it is unclear whether the role of VSR1 in the regulation of ABA biosynthesis requires the function of VSR1 in vacuolar trafficking. To determine whether VSR1 itself or its role in vacuolar trafficking is required for the osmotic stress response, *vrs1* mutants such as C2A:HA with minimum sequence changes but with a defect in vacuolar trafficking (Kim et al., 2010) would be very useful. The dominant-negative mutant (C2A:HA) has an Ala substitution in the C-terminal tail and displays inhibited vacuolar trafficking by interfering with endogenous VSR1 (Kim et al., 2010). Transgenic plants expressing the dominant-negative *vsr* mutant were more sensitive to osmotic stress and had lower expression of ABA biosynthesis genes relative to wild-type plants (Fig. 5, B and C). These data are therefore consistent with the notion that vacuolar trafficking mediated by VSR1 is required for ABA biosynthesis gene expression and osmotic stress resistance.

This study uncovered an unexpected link between vacuolar trafficking and ABA biosynthesis as well as stress signaling. There has been some other evidence to suggest that vacuolar trafficking machinery not only delivers cargo proteins to the vacuole, but also involves signal transduction and environmental stress responses (Surpin and Raikhel, 2004; Yamada et al., 2010; Andrés et al., 2014). For example, VSR3 is involved in ABA-mediated stomatal guard cell movement and has an important role in responses to plant stress (Avila et al., 2008). SNARE proteins have been suggested to contribute to the sensing of osmotic stress (Solsona et al., 1998). The vacuolar protein Vac14p regulates the levels of phosphatidylinositol 3,5-bisphosphate, which is an osmotic stress-induced phospholipid in yeast (*Saccharomyces cerevisiae*; Bonangelino et al., 2002). In Arabidopsis, the mutant *osmotic stress–sensitive mutant1* (*osm1*) was identified as an allele of the target-SNARE *Syntaxin of Plants61* (*SYP61*). The *osm1* mutant was sensitive to osmotic stress and soil drying and seemed to control stomatal response to ABA (Zhu et al., 2002). An Arabidopsis mutant in the SYP41-interacting protein Tonneau1 is also sensitive to salt and osmotic stress, possibly due to the mislocalization of SYP61 (Kim and Bassham, 2011). The antisense plants of Arabidopsis Vesicle-Associated Membrane Protein 7C showed improved salt tolerance through maintaining ΔpH and reducing vacuolar calcium release (Leshem et al., 2006). In addition, our microarray analysis of the *ced2* mutant revealed a key role of VSR1 in regulating the transcriptional network under osmotic stress. There are 2,559 genes that exhibited significantly altered expression in the *ced2* mutant under osmotic stress conditions. Among the down-regulated genes, a larger number were osmotic stress- or ABA-inducible genes, including those involved in ABA biosynthesis and signaling, and those encoding osmotic stress-responsive transcription factors, protein kinases, and other proteins (Fig. 4; Supplemental Tables S1 and S2). Thus, *VSR1* is likely to enable abiotic stress responses and does so, at least in part, by regulating many osmotic stress-induced genes.

Plant vacuoles are primed for maintaining cell volume and cell turgor, regulating ion homeostasis, and intracellular pH (Marty, 1999). To understand the mechanisms of vacuolar trafficking in osmotic stress signaling, we investigated whether ion flux and pH gradients in vacuoles might be altered in *vsr* mutants. Using the membrane potential dye bis-(1,3-dibarbituric acid)-trimethine oxanol (Konrad and Hedrich, 2008), we found that the membranes of *ced2*, *vsr1/vsr3*, and *vsr1/vsr4* mutants were more depolarized relative to those of the wild-type plants under osmotic stress (Fig. 6, A and B). Membrane depolarization has been observed in response to abiotic stress, such as hypoosmotic stress, cold stress, and salt stress (Covic et al., 1999; Lew, 2004; Carpaneto et al., 2007). It has been established that changes in the electrophysiological properties of the plasma membrane and vacuole membrane occurred prior to changes in gene expression in response to hyperosmotic stress (Covic et al., 1999; Lew, 2004). In the case of hyperosmotic shock, the cytoplasm and vacuole should remain at the same osmotic potential to avoid volume changes, which is required for vacuole and plasma membrane ion fluxes (Lew, 2004). Osmotic stress is likely to lead to transient change of cytosolic $Ca^{2+}$ fluxes that, in turn, may trigger downstream plant defense responses. Studies also implicate $[Ca^{2+}]_{cyt}$ as a second messenger involved in regulating ABA response and ABA biosynthesis (Knight et al., 1996; Pandey et al., 2004; Zou et al., 2010). In *ced2/vsr1* mutants, $[Ca^{2+}]_{cyt}$

was higher upon the osmotic stress treatment, which is consistent with more depolarized membrane potentials in the mutant. Moreover, in coordination with changes in $[Ca^{2+}]_{cyt}$, protons could also serve as a messenger molecule to activate downstream plant defense responses. Both these processes depend primarily on the ability of proton pumps in maintaining the pH gradients. The $H^+$-translocating enzymes ($H^+$-pumps) and cation/$H^+$ exchangers have been recognized to maintain optimal ion flux and pH gradients essential for cell function and plant adaption to stress. In plant cells, there are three types of $H^+$ pumps: P-type, V-type, and pyrophosphatase. After being synthesized in the ER, these proteins are targeted to diverse locations, including the plasma membrane, tonoplast, Golgi, and endosomes. The P-type $H^+$-adenosine triphosphatases are thought to function exclusively at the plasma membrane in the acidification of the cytoplasm, while the V-type and pyrophosphatase pumps are located on the tonoplast membrane and are thought to function primarily in the acidification of vacuoles. However, unlike in yeast and animals, at least one of the plant P-type $H^+$-adenosine triphosphatases (AHA10) may also contribute to the acidification of the endosome or vacuolar compartments (Baxter et al., 2005). Microarray analysis revealed that the expression level of several $H^+$-pumps and cation/$H^+$ exchangers was significantly lower in the *ced2* mutant than in the wild type in response to osmotic stress. These genes include *AHA4*, *AHA8*, *AHA10*, *CATION/H$^+$ EXCHANGER19* (*CHX19*), and *CHX23* (Fig. 4C). While the AHA proteins are well known to function in maintaining pH homeostasis (Sze et al., 1999), the cation/$H^+$ exchangers also appear to play a role in osmoregulation through $K^+$ fluxes and pH regulation (Padmanaban et al., 2007; Bassil et al., 2011; Barragán et al., 2012). The *vsr* mutants (*ced2*, *vsr1/vsr3*, and *vsr1/vsr4*) had a higher $pH_{vac}$ than the wild type in response to PEG-induced osmotic stress treatment (Fig. 6, E and F), suggesting that the overall capacity of the proton pump is reduced, and this is consistent with the reduced transcript levels of $H^+$-pumps and cation/$H^+$ exchanger-encoding genes in the mutant. Alternatively, these proton pumps, particularly the V-ATPases and tonoplast-localized cation/$H^+$ exchangers, may not be correctly targeted, and this, in turn, would compromise their activities in *vsr* mutants. In any event, a compromised regulation of the cellular pH homeostasis is likely a major cause for the aberrant ABA biosynthesis under osmotic stress.

To answer the question of whether osmotic stress-induced ABA biosynthesis is affected by intracellular pH changes, we used ConcA, a specific V-ATPase activity inhibitor, which has recently been shown to dramatically elevate pH in the $pH_{vac}$ and TGN but does not affect the pH of other endomembrane compartments (Krebs et al., 2010; Shen et al., 2013). ConcA treatment significantly decreased osmotic stress activation of NCED3 gene expression (Fig. 7A). We further employed mutants defective in V-ATPases to test their response to osmotic stress. V-ATPases are found at both the TGN and the tonoplast (Dettmer et al., 2006; Krebs et al., 2010). The *vha-a2/vha-a3* double mutants lack both tonoplast-localized A subunits, and thus V-ATPase activity on tonoplasts is reduced (Krebs et al., 2010), whereas the *det3* mutant lacks the TGN and early endosome-localized subunit C, and thus V-ATPase in both TGN and tonoplast is affected (Brüx et al., 2008). Our studies indicated that the reduced tonoplast V-ATPase activity by the *vha-a2/vha-a3* mutant does not significantly affect ABA biosynthesis under osmotic stress. By contrast, *det3*, which had reduced V-ATPase activity in the TGN, had impaired ABA biosynthesis (Fig. 7B; Supplemental Fig. S8). The reduced ABA biosynthesis in the *det3* mutant is consistent with the finding that inhibition of the TGN-localized V-ATPases leads to increase salt sensitivity and growth defects in plants (Batelli et al., 2007). It remains to be determined if $pH_{vac}$ was directly affected by TGN-localized V-ATPases or indirectly affected by reduced trafficking of proton pumps or other transporters. Our studies further revealed that osmotic stress-induced ABA biosynthesis is affected by disturbed intracellular pH homeostasis because changes in the $pH_{cyt}$ affect ABA biosynthesis (Fig. 7, C and D).

It is known that drought stress and ABA can lead to cytosolic alkalization in plant cells, including guard cells (Gehring et al., 1990; Irving et al., 1992; Blatt and Armstrong, 1993). Our data indicate that $pH_{cyt}$, in turn, regulates ABA biosynthesis and osmotic stress responses. However, the output (e.g. ABA biosynthesis) of this apparent loop or signaling cascade does not seem to linearly correlate with the absolute pH value in any compartments. Rather, it seems that ABA biosynthesis gene expression and ABA production depend more on the gradient between the cytoplasm and TGN/Early Endosome or the vacuole generated by the V-ATPases. Our data showed that acidification of the cytoplasm or alkalization of the vacuoles/TGN will diminish osmotic stress-activated ABA biosynthesis. Conversely, alkalization of the cytoplasm or acidification of the vacuoles/TGN will boost ABA biosynthesis. This regulation of the ABA biosynthesis may happen at several levels, including transcription and translation, and it is also conceivable that the catalytic activities of enzymes in the biosynthetic pathway or components in the signaling pathway are directly or indirectly modulated by pH changes within the range reported here. CED2/VSR1 is likely to have a role in regulating pH homeostasis via the targeting of vacuolar proton gradient generators to enable pH and osmotic stress-induced ABA biosynthesis.

In conclusion, our genetic, physiological, and molecular evidence provided in this study demonstrates that vacuolar trafficking mediated by VSRs is required for osmotic stress regulation of ABA biosynthesis genes and osmotic stress and drought stress resistance. We propose that changes of pH gradients between cytoplasm and vacuoles or other endosomal compartments may act as an early osmotic stress signal essential for the optimal induction of ABA biosynthesis and ABA-dependent signaling (Fig. 7E).

## MATERIALS AND METHODS

### Plant Materials and Map-Based Cloning

Arabidopsis (*Arabidopsis thaliana*) plants were grown at 21°C ± 1°C under continuous white light. Both wild-type (Col-*glabrous1*) and *ced2* mutant plants carried a homozygous *NCED3 promoter drived-luciferase* reporter gene (Wang et al., 2011). All other mutants are in the Col-0 background. T-DNA insertion lines of *vsr2*, *vsr4*, *vsr5*, *vsr6*, and *vsr7* were obtained from the SALK T-DNA insertion collection. *vsr1-2*, *vsr1-3*, and *vsr1-5* were gifts from Dr. Ikuko Hara-Nishimura. *VSR1*-HA, *C2A*:HA *4-3*, and *C2A*:HA *7-6* were gifts from Dr. Inhwan Hwang. *vsr3*, *vsr1/vsr3*, *vsr1/vsr4*, and *vsr5/vsr6* were gifts from Dr. Enrique Rojo. *vha-a2/vha-a3* and *det3* mutant lines were gifts from Dr. Karin Schumacher.

For map-based cloning, the *ced2* mutant was crossed with the Landsberg *erecta* accession, and 590 mutant plants were chosen from the F2 generation by their osmotic stress sensitivity phenotypes. All candidate genes in the fine-mapped interval were sequenced to identify the *ced2* mutation. The *VSR1* genomic fragment was cloned into pGWB501 and transformed into *ced2* for a complementation test.

### Stress Treatment

For germination test, seeds were sown on plates containing either a one-half-strength Murashige and Skoog (MS) medium (solidified with 1.5% [w/v] agar) with 2% (w/v) Suc buffered with 2 mM MES or the same medium supplemented with ABA or infused with PEG (average $M_r$, 8,000). For seedling growth, 4-d-old seedlings grown on vertically placed MS plates were transferred to the stress treatment plate for the indicated days. For water loss treatment, soil-grown plants were pretreated with or without 50 $\mu$m ABA for 4 h, and fully expanded leaves were then detached and incubated on the bench. The sample (consisting of four leaves) was weighed at the indicated time, and the loss of fresh weight was calculated as water loss.

### Determination of ABA Content

ABA contents were measured as described before (Wang et al., 2011). ABA was extracted by suspending 100 mg of lyophilized tissues in 1 mL of water and agitating overnight at 4°C. The ABA content was then determined with a Phytodetek ABA enzyme immunoassay test kit (Agdia).

### Ion Leakage Assay

For the PEG-induced ion leakage assay, 2-week-old seedlings were placed on plates with filter paper saturated with 40% (w/v) PEG. Seedlings were briefly washed with 0.3 M mannitol solution to remove the PEG solution and immediately placed in glass test tubes containing 10 mL of deionized water. The tubes containing the samples were shaken overnight, and the conductivity was measured (Xiong et al., 2001b).

### Stomatal Aperture Measurement

Stomatal aperture measurement was performed as described (Chitrakar and Melotto, 2010). Rosette leaves were immersed in the 20 $\mu$M propidium iodide (P4864, Sigma) solution for 5 min and rinsed with distilled water. Then, leaves were incubated in a stomatal open solution (10 mM KCl, 50 $\mu$M $CaCl_2$, and 10 mM MES-KOH, pH 6.15) for 3 h before ABA was added. To study ABA-mediated inhibition of light-induced stomatal opening, plants were kept in darkness for 24 h to close the stomata before staining and then kept under light in solution with ABA addition. Images were obtained with a laser scanning confocal microscope (LSM 710, Carl Zeiss) with excitation and emission wavelengths of 458 and 543 to 620 nm, respectively. At least 120 stomata for each treatment were measured using the laser scanning confocal microscope image browser.

### RNA Gel Analysis and Reverse Transcription-PCR Analysis

RNA gel-blot analysis was performed as described (Wang et al., 2011). Total RNA from seedlings was extracted with the Trizol reagent (Invitrogen) and reversed transcribed using SuperScript III First-Strand Synthesis Supermix (Invitrogen). All the reactions were performed with the 7900HT Fast Real-Time PCR System (Applied Biosystems). Each experiment was replicated three times. The primers used in this study are listed in Supplemental Table S3.

### Microarray Analysis

The probe preparation, hybridization to the Arabidopsis ATH1 gene expression arrays (Agilent Technologies), and subsequent processing steps were performed according to the manufacturer's procedures. After hybridization, raw signals were extracted from the scanned microarray slides, and data were analyzed using the Feature Extraction Software (10.7.1.1, Agilent Technologies) with the default settings. These signals were then $\log_2$ transformed and subjected to percentile shift-based normalization and median-based baseline transformation using Genespring GX (Agilent Technologies), where the Benjamini-Hochberg false discovery rates were used to analyze significance, and genes with fold changes of at least 2 and a false discovery rate-corrected *P* value lower than 0.05 were identified.

### Detection of ROS, Membrane Potential, Calcium Flux, and $pH_{vac}$

For ROS production, seedlings were stained by $H_2$DCF-DA following the indicated stress treatment. The image was captured with the LSM 710 confocal microscope (excitation at 488 nm and emission at 525 nm). For membrane potential, seedlings were stained with bis-(1,3-dibutylbarbituric acid) trimethine oxonol (Invitrogen) for 1 h and rinsed three times with distilled water before stress treatment. The stained seedlings were then mounted on cover slides, 40% (w/v) PEG solution was applied, and the fluorescence was monitored. Images were captured using the LSM 710 (excitation at 488 nm and emission at 530 ± 15 nm). For visualizing $Ca^{2+}$, 20 $\mu$M Fluo-4-AM was loaded in the presence of 0.02% (v/v) pluronic F-127 (P3000MP, Invitrogen) and incubated for 2 h with gentle shaking. Images from the stained seedlings were captured using the LSM 710 confocal microscope (excitation at 488 nm and emission at 520 nm) after PEG treatment for the indicated time. The fluorescence intensity was analyzed using the ZEN 2009 software. For $pH_{vac}$ measurement, seedlings were stained with pH-sensitive dye BCECF-AM (B-1150, Invitrogen). Dye loading was performed as described (Bassil et al., 2011) with minor modifications. Briefly, seedlings were incubated in one-tenth-strength MS liquid medium (0.5% [w/v] Suc and 10 mM MES, pH 5.7) containing 10 $\mu$M BCECF-AM and 0.02% (v/v) pluronic F-127 (P3000MP, Invitrogen) for 1 h in darkness at 22°C and washed twice with one-tenth-strength MS buffer before stress treatments. The stained seedlings were incubated in 40% (w/v) PEG or 50 $\mu$M ABA for 1 h. The images were obtained using the LSM 710 confocal microscope (excitation at 458 and 488 nm and emission at 525–550 nm). After background correction, the integrated pixel intensity was measured for both the 458 nm-excited images and the 488 nm-excited images, and ratios were calculated with ImageJ (version 1.46, National Institutes of Health). Fluorescence ratios were used to calculate the pH from a calibration curve. For pH calibration, 7-d-old seedlings were incubated for 15 min in equilibration buffers containing 50 mM 1,3-bis(tris[hydroxymethyl]methylamino) propane-HEPES or MES (pH varied from 5.2–7.4) and 50 mM ammonium acetate. The fluorescence images were obtained, and ratios were calculated as described above. A calibration curve was made between the fluorescence ratios and the corresponding pH values.

Sequence data from this article can be found in the GenBank/EMBL data libraries under accession numbers *VSR1/CED2* (At3g52850), *NCED3* (At3g14440), *ABA1* (At5g67030), *AAO3* (At2g27150), *ABF2* (At1G45249), *NF-YA5* (At1G54160), *ABI5* (At2G36270), *GORK* (At5G37500), *FAB1B* (AT3G14270), *AHA4* (AT3G47950), *AHA8* (AT3G42640), *AHA10* (AT1G17260), *PUB22* (At3G52450), *PUB23* (At2G35930), and *HKT1* (At4G10310). The microarray data discussed in this publication have been deposited in the National Center for Biotechnology Information's Gene Expression Omnibus and are accessible through Gene Expression Omnibus Series accession number (http://www.ncbi.nlm.nih.gov/geo/query/acc.cgi?acc=GSE44419).

### Supplemental Data

The following supplemental materials are available.

**Supplemental Figure S1.** Characterization of the *ced2* mutant.

**Supplemental Figure S2.** Sensitivity of the *ced2* mutant to salt stress.

**Supplemental Figure S3.** *VSR1* expression is partly dependent on ABA.

**Supplemental Figure S4.** Water loss rate and drought tolerance of the *ced2* mutant.

**Supplemental Figure S5.** Gene ontology of genes with altered expression in *ced2* under osmotic stress conditions.

**Supplemental Figure S6.** Characterization of other *vsr* mutants.

**Supplemental Figure S7.** Membrane potential and vacuolar pH.

**Supplemental Figure S8.** ABA accumulation in *det3* and *vha-a2/vha-a3* mutants.

## ACKNOWLEDGMENTS

We thank Drs. Ikuko Hara-Nishimura, Inhwan Hwang, Enrique Rojo, and Karin Schumacher for providing Arabidopsis mutants, Dr. Paul E. Verslues for initial mutant screening, and Rebecca Stevenson for technical assistance.

Received August 24, 2014; accepted November 19, 2014; published November 21, 2014.

## LITERATURE CITED

**Andrés Z, Pérez-Hormaeche J, Leidi EO, Schlücking K, Steinhorst L, McLachlan DH, Schumacher K, Hetherington AM, Kudla J, Cubero B, et al** (2014) Control of vacuolar dynamics and regulation of stomatal aperture by tonoplast potassium uptake. Proc Natl Acad Sci USA **111:** E1806–E1814

**Avila EL, Brown M, Pan S, Desikan R, Neill SJ, Girke T, Surpin M, Raikhel NV** (2008) Expression analysis of Arabidopsis vacuolar sorting receptor 3 reveals a putative function in guard cells. J Exp Bot **59:** 1149–1161

**Barragán V, Leidi EO, Andrés Z, Rubio L, De Luca A, Fernández JA, Cubero B, Pardo JM** (2012) Ion exchangers NHX1 and NHX2 mediate active potassium uptake into vacuoles to regulate cell turgor and stomatal function in *Arabidopsis*. Plant Cell **24:** 1127–1142

**Bassil E, Tajima H, Liang YC, Ohto MA, Ushijima K, Nakano R, Esumi T, Coku A, Belmonte M, Blumwald E** (2011) The Arabidopsis $Na^+/H^+$ antiporters NHX1 and NHX2 control vacuolar pH and $K^+$ homeostasis to regulate growth, flower development, and reproduction. Plant Cell **23:** 3482–3497

**Batelli G, Verslues PE, Agius F, Qiu Q, Fujii H, Pan S, Schumaker KS, Grillo S, Zhu JK** (2007) SOS2 promotes salt tolerance in part by interacting with the vacuolar $H^+$-ATPase and upregulating its transport activity. Mol Cell Biol **27:** 7781–7790

**Baxter IR, Young JC, Armstrong G, Foster N, Bogenschutz N, Cordova T, Peer WA, Hazen SP, Murphy AS, Harper JF** (2005) A plasma membrane $H^+$-ATPase is required for the formation of proanthocyanidins in the seed coat endothelium of *Arabidopsis thaliana*. Proc Natl Acad Sci USA **102:** 2649–2654

**Bibikova TN, Jacob T, Dahse I, Gilroy S** (1998) Localized changes in apoplastic and cytoplasmic pH are associated with root hair development in *Arabidopsis thaliana*. Development **125:** 2925–2934

**Blatt M, Armstrong F** (1993) $K^+$ channels of stomatal guard cells: abscisic-acid-evoked control of the outward rectifier mediated by cytoplasmic pH. Planta **191:** 330–341

**Bonangelino CJ, Nau JJ, Duex JE, Brinkman M, Wurmser AE, Gary JD, Emr SD, Weisman LS** (2002) Osmotic stress-induced increase of phosphatidylinositol 3,5-bisphosphate requires Vac14p, an activator of the lipid kinase Fab1p. J Cell Biol **156:** 1015–1028

**Brüx A, Liu TY, Krebs M, Stierhof YD, Lohmann JU, Miersch O, Wasternack C, Schumacher K** (2008) Reduced V-ATPase activity in the *trans*-Golgi network causes oxylipin-dependent hypocotyl growth inhibition in *Arabidopsis*. Plant Cell **20:** 1088–1100

**Carpaneto A, Ivashikina N, Levchenko V, Krol E, Jeworutzki E, Zhu JK, Hedrich R** (2007) Cold transiently activates calcium-permeable channels in Arabidopsis mesophyll cells. Plant Physiol **143:** 487–494

**Castelli S, Vitale A** (2005) The phaseolin vacuolar sorting signal promotes transient, strong membrane association and aggregation of the bean storage protein in transgenic tobacco. J Exp Bot **56:** 1379–1387

**Chen Z, Zhang H, Jablonowski D, Zhou X, Ren X, Hong X, Schaffrath R, Zhu JK, Gong Z** (2006) Mutations in ABO1/ELO2, a subunit of holo-Elongator, increase abscisic acid sensitivity and drought tolerance in *Arabidopsis thaliana*. Mol Cell Biol **26:** 6902–6912

**Chitrakar R, Melotto M** (2010) Assessing stomatal response to live bacterial cells using whole leaf imaging. J Vis Exp **44:** e2185

**Covic L, Silva NF, Lew RR** (1999) Functional characterization of ARAKIN (ATMEKK1): a possible mediator in an osmotic stress response pathway in higher plants. Biochim Biophys Acta **1451:** 242–254

**Cutler S, Ghassemian M, Bonetta D, Cooney S, McCourt P** (1996) A protein farnesyl transferase involved in abscisic acid signal transduction in Arabidopsis. Science **273:** 1239–1241

**Cutler SR, Rodriguez PL, Finkelstein RR, Abrams SR** (2010) Abscisic acid: emergence of a core signaling network. Annu Rev Plant Biol **61:** 651–679

**daSilva LL, Taylor JP, Hadlington JL, Hanton SL, Snowden CJ, Fox SJ, Foresti O, Brandizzi F, Denecke J** (2005) Receptor salvage from the prevacuolar compartment is essential for efficient vacuolar protein targeting. Plant Cell **17:** 132–148

**Dettmer J, Hong-Hermesdorf A, Stierhof YD, Schumacher K** (2006) Vacuolar $H^+$-ATPase activity is required for endocytic and secretory trafficking in *Arabidopsis*. Plant Cell **18:** 715–730

**Dodd AN, Kudla J, Sanders D** (2010) The language of calcium signaling. Annu Rev Plant Biol **61:** 593–620

**Finkelstein RR, Gibson SI** (2002) ABA and sugar interactions regulating development: cross-talk or voices in a crowd? Curr Opin Plant Biol **5:** 26–32

**Foresti O, daSilva LL, Denecke J** (2006) Overexpression of the *Arabidopsis* syntaxin PEP12/SYP21 inhibits transport from the prevacuolar compartment to the lytic vacuole in vivo. Plant Cell **18:** 2275–2293

**Foresti O, Gershlick DC, Bottanelli F, Hummel E, Hawes C, Denecke J** (2010) A recycling-defective vacuolar sorting receptor reveals an intermediate compartment situated between prevacuoles and vacuoles in tobacco. Plant Cell **22:** 3992–4008

**Fuji K, Shimada T, Takahashi H, Tamura K, Koumoto Y, Utsumi S, Nishizawa K, Maruyama N, Hara-Nishimura I** (2007) *Arabidopsis* vacuolar sorting mutants (green fluorescent seed) can be identified efficiently by secretion of vacuole-targeted green fluorescent protein in their seeds. Plant Cell **19:** 597–609

**Fujii H, Verslues PE, Zhu JK** (2007) Identification of two protein kinases required for abscisic acid regulation of seed germination, root growth, and gene expression in *Arabidopsis*. Plant Cell **19:** 485–494

**Fujita Y, Yoshida T, Yamaguchi-Shinozaki K** (2013) Pivotal role of the AREB/ABF-SnRK2 pathway in ABRE-mediated transcription in response to osmotic stress in plants. Physiol Plant **147:** 15–27

**Gehring CA, Irving HR, Parish RW** (1990) Effects of auxin and abscisic acid on cytosolic calcium and pH in plant cells. Proc Natl Acad Sci USA **87:** 9645–9649

**Herman EM, Li X, Su RT, Larsen P, Hsu H, Sze H** (1994) Vacuolar-type $H^+$-ATPases are associated with the endoplasmic reticulum and provacuoles of root tip cells. Plant Physiol **106:** 1313–1324

**Hruz T, Laule O, Szabo G, Wessendorp F, Bleuler S, Oertle L, Widmayer P, Gruissem W, Zimmermann P** (2008) Genevestigator v3: a reference expression database for the meta-analysis of transcriptomes. Adv Bioinforma **2008:** 420747

**Hugouvieux V, Kwak JM, Schroeder JI** (2001) An mRNA cap binding protein, ABH1, modulates early abscisic acid signal transduction in Arabidopsis. Cell **106:** 477–487

**Irving HR, Gehring CA, Parish RW** (1992) Changes in cytosolic pH and calcium of guard cells precede stomatal movements. Proc Natl Acad Sci USA **89:** 1790–1794

**Iuchi S, Kobayashi M, Taji T, Naramoto M, Seki M, Kato T, Tabata S, Kakubari Y, Yamaguchi-Shinozaki K, Shinozaki K** (2001) Regulation of drought tolerance by gene manipulation of 9-*cis*-epoxycarotenoid dioxygenase, a key enzyme in abscisic acid biosynthesis in Arabidopsis. Plant J **27:** 325–333

**Iuchi S, Kobayashi M, Yamaguchi-Shinozaki K, Shinozaki K** (2000) A stress-inducible gene for 9-cis-epoxycarotenoid dioxygenase involved in abscisic acid biosynthesis under water stress in drought-tolerant cowpea. Plant Physiol **123:** 553–562

**Kim H, Kang H, Jang M, Chang JH, Miao Y, Jiang L, Hwang I** (2010) Homomeric interaction of AtVSR1 is essential for its function as a vacuolar sorting receptor. Plant Physiol **154:** 134–148

**Kim SJ, Bassham DC** (2011) TNO1 is involved in salt tolerance and vacuolar trafficking in Arabidopsis. Plant Physiol **156:** 514–526

**Knight H, Trewavas AJ, Knight MR** (1996) Cold calcium signaling in *Arabidopsis* involves two cellular pools and a change in calcium signature after acclimation. Plant Cell **8:** 489–503

**Konrad KR, Hedrich R** (2008) The use of voltage-sensitive dyes to monitor signal-induced changes in membrane potential-ABA triggered membrane depolarization in guard cells. Plant J **55:** 161–173

**Krebs M, Beyhl D, Görlich E, Al-Rasheid KA, Marten I, Stierhof YD, Hedrich R, Schumacher K** (2010) Arabidopsis V-ATPase activity at the tonoplast is required for efficient nutrient storage but not for sodium accumulation. Proc Natl Acad Sci USA **107:** 3251–3256

**Lee Y, Jang M, Song K, Kang H, Lee MH, Lee DW, Zouhar J, Rojo E, Sohn EJ, Hwang I** (2013) Functional identification of sorting receptors

involved in trafficking of soluble lytic vacuolar proteins in vegetative cells of Arabidopsis. Plant Physiol **161:** 121–133

**Leshem Y, Melamed-Book N, Cagnac O, Ronen G, Nishri Y, Solomon M, Cohen G, Levine A** (2006) Suppression of Arabidopsis vesicle-SNARE expression inhibited fusion of $H_2O_2$-containing vesicles with tonoplast and increased salt tolerance. Proc Natl Acad Sci USA **103:** 18008–18013

**Lew RR** (2004) Osmotic effects on the electrical properties of Arabidopsis root hair vacuoles in situ. Plant Physiol **134:** 352–360

**Marty F** (1999) Plant vacuoles. Plant Cell **11:** 587–600

**Mustilli AC, Merlot S, Vavasseur A, Fenzi F, Giraudat J** (2002) *Arabidopsis* OST1 protein kinase mediates the regulation of stomatal aperture by abscisic acid and acts upstream of reactive oxygen species production. Plant Cell **14:** 3089–3099

**Nakamura N, Tanaka S, Teko Y, Mitsui K, Kanazawa H** (2005) Four $Na^+/H^+$ exchanger isoforms are distributed to Golgi and post-Golgi compartments and are involved in organelle pH regulation. J Biol Chem **280:** 1561–1572

**Nambara E, Marion-Poll A** (2005) Abscisic acid biosynthesis and catabolism. Annu Rev Plant Biol **56:** 165–185

**Niemes S, Labs M, Scheuring D, Krueger F, Langhans M, Jesenofsky B, Robinson DG, Pimpl P** (2010) Sorting of plant vacuolar proteins is initiated in the ER. Plant J **62:** 601–614

**Padmanaban S, Chanroj S, Kwak JM, Li X, Ward JM, Sze H** (2007) Participation of endomembrane cation/$H^+$ exchanger AtCHX20 in osmoregulation of guard cells. Plant Physiol **144:** 82–93

**Pandey GK, Cheong YH, Kim KN, Grant JJ, Li L, Hung W, D'Angelo C, Weinl S, Kudla J, Luan S** (2004) The calcium sensor calcineurin B-like 9 modulates abscisic acid sensitivity and biosynthesis in *Arabidopsis*. Plant Cell **16:** 1912–1924

**Pardo JM, Cubero B, Leidi EO, Quintero FJ** (2006) Alkali cation exchangers: roles in cellular homeostasis and stress tolerance. J Exp Bot **57:** 1181–1199

**Qin X, Zeevaart JA** (1999) The 9-*cis*-epoxycarotenoid cleavage reaction is the key regulatory step of abscisic acid biosynthesis in water-stressed bean. Proc Natl Acad Sci USA **96:** 15354–15361

**Qin X, Zeevaart JA** (2002) Overexpression of a 9-cis-epoxycarotenoid dioxygenase gene in *Nicotiana plumbaginifolia* increases abscisic acid and phaseic acid levels and enhances drought tolerance. Plant Physiol **128:** 544–551

**Ren X, Chen Z, Liu Y, Zhang H, Zhang M, Liu Q, Hong X, Zhu JK, Gong Z** (2010) ABO3, a WRKY transcription factor, mediates plant responses to abscisic acid and drought tolerance in Arabidopsis. Plant J **63:** 417–429

**Romani G, Pallini S, Beffagna N** (1998) Down-regulation of the plasmalemma $H^+$ pump activity by nicotine-induced intracellular alkalinization: a balance between base accumulation, biochemical pH-stat response and intracellular pH increase. Plant Cell Physiol **39:** 169–176

**Schumacher K, Vafeados D, McCarthy M, Sze H, Wilkins T, Chory J** (1999) The Arabidopsis *det3* mutant reveals a central role for the vacuolar $H^+$-ATPase in plant growth and development. Genes Dev **13:** 3259–3270

**Shen J, Zeng Y, Zhuang X, Sun L, Yao X, Pimpl P, Jiang L** (2013) Organelle pH in the Arabidopsis endomembrane system. Mol Plant **6:** 1419–1437

**Shimada T, Fuji K, Tamura K, Kondo M, Nishimura M, Hara-Nishimura I** (2003) Vacuolar sorting receptor for seed storage proteins in *Arabidopsis thaliana*. Proc Natl Acad Sci USA **100:** 16095–16100

**Solsona C, Innocenti B, Fernández JM** (1998) Regulation of exocytotic fusion by cell inflation. Biophys J **74:** 1061–1073

**Surpin M, Raikhel N** (2004) Traffic jams affect plant development and signal transduction. Nat Rev Mol Cell Biol **5:** 100–109

**Sze H, Li X, Palmgren MG** (1999) Energization of plant cell membranes by $H^+$-pumping ATPases regulation and biosynthesis. Plant Cell **11:** 677–690

**Sze H, Liang F, Hwang I, Curran AC, Harper JF** (2000) Diversity and regulation of plant $Ca^{2+}$ pumps: insights from expression in yeast. Annu Rev Plant Physiol Plant Mol Biol **51:** 433–462

**Tan BC, Joseph LM, Deng WT, Liu L, Li QB, Cline K, McCarty DR** (2003) Molecular characterization of the Arabidopsis 9-*cis* epoxycarotenoid dioxygenase gene family. Plant J **35:** 44–56

**Tan BC, Schwartz SH, Zeevaart JA, McCarty DR** (1997) Genetic control of abscisic acid biosynthesis in maize. Proc Natl Acad Sci USA **94:** 12235–12240

**Thompson AJ, Jackson AC, Symonds RC, Mulholland BJ, Dadswell AR, Blake PS, Burbidge A, Taylor IB** (2000) Ectopic expression of a tomato 9-*cis*-epoxycarotenoid dioxygenase gene causes over-production of abscisic acid. Plant J **23:** 363–374

**Wang D, Weaver ND, Kesarwani M, Dong X** (2005) Induction of protein secretory pathway is required for systemic acquired resistance. Science **308:** 1036–1040

**Wang ZY, Xiong L, Li W, Zhu JK, Zhu J** (2011) The plant cuticle is required for osmotic stress regulation of abscisic acid biosynthesis and osmotic stress tolerance in *Arabidopsis*. Plant Cell **23:** 1971–1984

**Xiong L, Gong Z, Rock CD, Subramanian S, Guo Y, Xu W, Galbraith D, Zhu JK** (2001a) Modulation of abscisic acid signal transduction and biosynthesis by an Sm-like protein in Arabidopsis. Dev Cell **1:** 771–781

**Xiong L, Ishitani M, Lee H, Zhu JK** (2001b) The *Arabidopsis LOS5/ABA3* locus encodes a molybdenum cofactor sulfurase and modulates cold stress- and osmotic stress-responsive gene expression. Plant Cell **13:** 2063–2083

**Xiong L, Lee H, Ishitani M, Zhu JK** (2002) Regulation of osmotic stress-responsive gene expression by the *LOS6/ABA1* locus in Arabidopsis. J Biol Chem **277:** 8588–8596

**Xiong L, Zhu JK** (2003) Regulation of abscisic acid biosynthesis. Plant Physiol **133:** 29–36

**Yamada K, Osakabe Y, Mizoi J, Nakashima K, Fujita Y, Shinozaki K, Yamaguchi-Shinozaki K** (2010) Functional analysis of an *Arabidopsis thaliana* abiotic stress-inducible facilitated diffusion transporter for monosaccharides. J Biol Chem **285:** 1138–1146

**Yoshida R, Hobo T, Ichimura K, Mizoguchi T, Takahashi F, Aronso J, Ecker JR, Shinozaki K** (2002) ABA-activated SnRK2 protein kinase is required for dehydration stress signaling in Arabidopsis. Plant Cell Physiol **43:** 1473–1483

**Zhang X, Dong FC, Gao JF, Song CP** (2001) Hydrogen peroxide-induced changes in intracellular pH of guard cells precede stomatal closure. Cell Res **11:** 37–43

**Zhu J, Gong Z, Zhang C, Song CP, Damsz B, Inan G, Koiwa H, Zhu JK, Hasegawa PM, Bressan RA** (2002) OSM1/SYP61: a syntaxin protein in *Arabidopsis* controls abscisic acid-mediated and non-abscisic acid-mediated responses to abiotic stress. Plant Cell **14:** 3009–3028

**Zhu JK** (2002) Salt and drought stress signal transduction in plants. Annu Rev Plant Biol **53:** 247–273

**Zou JJ, Wei FJ, Wang C, Wu JJ, Ratnasekera D, Liu WX, Wu WH** (2010) Arabidopsis calcium-dependent protein kinase CPK10 functions in abscisic acid- and $Ca^{2+}$-mediated stomatal regulation in response to drought stress. Plant Physiol **154:** 1232–1243

**Zouhar J, Muñoz A, Rojo E** (2010) Functional specialization within the vacuolar sorting receptor family: VSR1, VSR3 and VSR4 sort vacuolar storage cargo in seeds and vegetative tissues. Plant J **64:** 577–588